REVIEWS AND SYNTHESES

Transmission assumptions generate conflicting predictions in host–vector disease models: a case study in West Nile virus

Marjorie J. Wonham,[1]* Mark A. Lewis,[1] Joanna Rencławowicz[1,2,3] and P. van den Driessche[2]

[1]*Department of Biological Sciences and Department of Mathematical and Statistical Sciences, Centre for Mathematical Biology, University of Alberta, CAB 632, Edmonton, AB, Canada T6G 2G1*
[2]*Department of Mathematics and Statistics, University of Victoria, Victoria, BC, Canada V8W 3P4*
[3]*Institute of Mathematics, Polish Academy of Sciences, Sniadeckich 8, 00-956 Warsaw, Poland*
Correspondence: E-mail: mwonham@ualberta.ca

Abstract

This review synthesizes the conflicting outbreak predictions generated by different biological assumptions in host–vector disease models. It is motivated by the North American outbreak of West Nile virus, an emerging infectious disease that has prompted at least five dynamical modelling studies. Mathematical models have long proven successful in investigating the dynamics and control of infectious disease systems. The underlying assumptions in these epidemiological models determine their mathematical structure, and therefore influence their predictions. A crucial assumption is the host–vector interaction encapsulated in the disease-transmission term, and a key prediction is the basic reproduction number, $\mathcal{R}_0$. We connect these two model elements by demonstrating how the choice of transmission term qualitatively and quantitatively alters $\mathcal{R}_0$ and therefore alters predicted disease dynamics and control implications. Whereas some transmission terms predict that reducing the host population will reduce disease outbreaks, others predict that this will exacerbate infection risk. These conflicting predictions are reconciled by understanding that different transmission terms apply biologically only at certain population densities, outside which they can generate erroneous predictions. For West Nile virus, $\mathcal{R}_0$ estimates for six common North American bird species indicate that all would be effective outbreak hosts.

Keywords:

Arboviral encephalitis, basic reproduction number, disease control, emerging infectious disease, $\mathcal{R}_0$, transmission dynamics, West Nile virus.

INTRODUCTION

Mathematical models have long provided important insight into disease dynamics and control (e.g. Anderson & May 1991; Hethcote 2000). As emerging and re-emerging infectious diseases increase in outbreak frequency, there is a compelling interest in understanding their dynamics (Daszak *et al.* 2000; Dobson & Foufopoulos 2001; Castillo-Chavez *et al.* 2002; Gubler 2002; Chomel 2003; Enserink 2004). In all disease modelling, a model's mathematical structure is determined by its underlying biological assumptions, which therefore influence the model's predictions. Here, we show how a central assumption in epidemiological modelling, the form of the disease-transmission term, affects a central prediction, the basic reproduction number. We also illustrate the effects of other epidemiological features on model predictions.

The disease-transmission term represents the contact between host individuals in directly transmitted diseases, or between host and vector individuals in host–vector diseases (see Fig. 1a). The choice of which transmission term to use has been extensively discussed, particularly for directly transmitted diseases (Getz & Pickering 1983; Anderson & May 1991; Thrall *et al.* 1993; McCallum *et al.* 2001; Begon *et al.* 2002; Keeling 2005; Rudolf & Antonovics 2005). However, the implications of this choice for disease prediction and control have received much less attention (e.g. Wood & Thomas 1999; McCallum *et al.* 2001).

A dynamical disease model generates the basic reproduction number, $\mathcal{R}_0$, which represents the average number of

(a) Reservoirs   Vectors
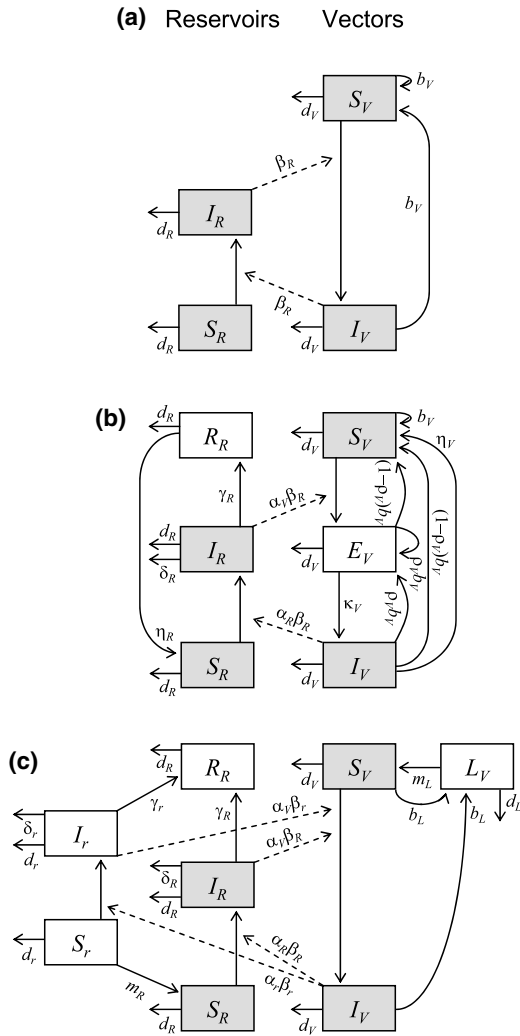
Figure 1 Flow diagrams of (a) the core West Nile virus model, (b) the core model with added epidemiological dynamics, and (c) the core model with added vital dynamics and population stage structure. Shaded boxes highlight the core model; solid lines indicate movement of individuals in and out of classes; dashed lines indicate disease transmission by mosquito bite. Variables and parameters are defined in Table 2.

secondary infections caused by the introduction of a typical infected individual into an otherwise entirely susceptible population (Anderson & May 1991; Heesterbeek 2002). This number serves as an invasion threshold both for predicting outbreaks and for evaluating control strategies. In recent epidemiological modelling, uncertainty and sensitivity analyses have been used to evaluate the effect of different model parameters on $\mathcal{R}_0$ for directly transmitted diseases (e.g. Blower & Dowlatabadi 1994; Sanchez & Blower 1997; Chowell *et al.* 2004). Again, however, the effect of transmission-term assumptions on $\mathcal{R}_0$ has only briefly been mentioned (McCallum *et al.* 2001), and has not been

quantitatively assessed. We connect these central two elements of disease modelling by showing how different transmission terms influence $\mathcal{R}_0$, both qualitatively and quantitatively. We focus on host–vector disease systems, in which the added complexity of two interacting populations introduces a wider range of model features. We also show how a range of assumptions about epidemiological features, species' parameter values, and life-history features influence $\mathcal{R}_0$.

Our analysis is motivated by a particular emerging infectious disease system, the North American outbreak of West Nile virus. This arboviral encephalitis amplifies in a transmission cycle between vector mosquitoes and reservoir birds, and is secondarily transmitted to mammals, including humans (Gubler *et al.* 2000; Bernard *et al.* 2001; Peterson *et al.* 2004). Since its initial North American report in New York City in 1999, West Nile virus has spread across the continent and prompted at least five dynamical mathematical modelling studies (Table 1). Although these models share a common structure, they differ in their biological assumptions and therefore in their predictions. To compare the effects of these different assumptions, we first develop a core model that contains the elements common to all the published models. We then systematically alter the core model to consider the qualitative and quantitative effects of different assumptions on $\mathcal{R}_0$. To gain further insight into this type of disease dynamic, we include in our review two similar models of other mosquito-borne pathogens, Japanese encephalitis and Ross River virus (Table 1).

West Nile virus models

All seven arboviral models reviewed here share a standard susceptible–infectious (S–I) structure for vector and host populations. Table 1 summarizes their key features, and the Appendix presents their equations and $\mathcal{R}_0$ expressions in a common notation. For simplicity, we abbreviate the models as follows: West Nile virus, WN1–5, Japanese encephalitis, JE, and Ross River virus, RR (Table 1). In an additional series of studies, Japanese and Murray Valley encephalitis and RR virus are modelled using a cyclic representation of vector feeding behaviour (Kay *et al.* 1987; Saul *et al.* 1990; Saul 2003; Glass 2005). However, as these models cannot readily be converted to a system of ordinary differential equations for comparison with the other seven, they are not included in our review.

CORE MODEL

The three central populations of an arboviral encephalitis system like West Nile virus are the arthropod vectors, reservoir hosts and secondary hosts (Gubler 2002). The dynamical behaviour of the disease is determined by the

Table 1 Comparison of seven dynamical models of mosquito-borne virus transmission

Disease system	West Nile virus					Japanese encephalitis	Ross River virus
Model	WN1[1]	WN2[2]	WN3[3]	WN4[4]	WN5[5]	JE[6]	RR[7]
No. equations	8 (4)	6 (3)	7 (3)	4 (2)	5 (2)	5 (2)	11 (5)
Disease classes							
Vector	S_V, E_V, I_V	S_V, E_V, I_V	L_V, S_V, E_V, I_V	S_V, I_V	S_V, I_V	S_V, I_V	$S_{V1}, E_{V1}, I_{V1}, R_{V1}, S_{V2}, E_{V2}, I_{V2}, R_{V2}$
Reservoir	S_R, S_r, I_R, I_r, R_R	S_R, I_R, R_R	S_R, I_R, R_R	S_R, I_R	S_R, I_R, R_R	S_R, I_R, R_R	S_R, I_R, R_R
Transmission dynamics	FR	MA	FR	FR	FR	FS	MA, C
Epidemiological features							
Transmission probabilities	Y	·	Y	Y	Y	Y	·
V viral incubation period	Y	Y	Y	·	·	·	Y
V loss of infectivity	·	·	·	·	·	Y	·
V vertical transmission	·	Y	·	·	Y	·	·
R death from virus	Y	·	Y	Y	Y	·	·
R recovery to immune	Y	Y	Y	·	Y	Y	Y
R loss of immunity	·	·	·	·	·	Y	·
Vital dynamics							
Vector	Y	Y	Y	Y	Y	Y	Y
Reservoir	Y	Y	·	Y	Y	Y	·
Age structure							
Vector	·	·	Y	·	·	·	·
Reservoir	Y	·	·	·	·	·	·

Classes for vectors (V) and reservoirs (adult R, juvenile r) determine the number of model equations, of which only the subset in parentheses contribute to the calculation of $\mathcal{R}_0$. Disease transmission functions are reservoir frequency dependence (FR), mass action (MA), susceptible frequency dependence (FS), and a constant rate from hosts outside the model (C). Inclusion of epidemiological and vital dynamics features indicated as Y, yes or ·, no.
Sources: [1]Lord & Day (2001a,b); [2]Thomas & Urena (2001) as converted to continuous time ODEs in Lewis *et al.* (2006b); [3]Wonham *et al.* (2004); [4]Bowman *et al.* (2005); [5]Cruz-Pacheco *et al.* (2005); [6]Tapaswi *et al.* (1995); [7]Choi *et al.* (2002).

vector and reservoir populations alone, from which the risk to secondary hosts may be inferred (but see Higgs *et al.* 2005).

The core vector–reservoir structure common to all seven arboviral models comprises four compartments: susceptible vectors (S_V) infectious vectors (I_V), susceptible reservoirs (S_R), and infectious reservoirs (I_R) (Fig. 1a). The vector equations describe the dynamics of adult female mosquitoes; the reservoir equations describe the dynamics primarily of birds for West Nile virus, and mammals for JE and RR virus. Cross-infection occurs when an infectious vector bites a susceptible reservoir or a susceptible vector bites an infectious reservoir. The mosquito lifecycle, which is on the order of 1 month, is represented by birth and death rates. For the bird lifecycle, which is one to two orders of magnitude longer, the birth and death rates are correspondingly lower and can reasonably be omitted for a single-season model. However, as the model requires at least one reservoir loss parameter, we begin with the natural death rate, which is used in all but two of the original models. (WN3 and RR use other loss terms.) The core model can be expressed as a system of four ordinary differential equations,

$$\underbrace{\frac{dS_V}{dt}}_{\text{Susceptible vectors}} = \underbrace{b_V N_V}_{\text{birth}} - \underbrace{\beta_R \frac{I_R}{N_R} S_V}_{\text{disease transmission}} - \underbrace{d_V S_V}_{\text{death}}$$

$$\underbrace{\frac{dI_V}{dt}}_{\text{Infectious vectors}} = \underbrace{\beta_R \frac{I_R}{N_R} S_V}_{\text{disease transmission}} - \underbrace{d_V I_V}_{\text{death}}$$

$$\underbrace{\frac{dS_R}{dt}}_{\text{Susceptible reservoirs}} = - \underbrace{\beta_R \frac{S_R}{N_R} I_V}_{\text{disease transmission}} - \underbrace{d_R S_R}_{\text{death}},$$

$$\underbrace{\frac{dI_R}{dt}}_{\text{Infectious reservoirs}} = \underbrace{\beta_R \frac{S_R}{N_R} I_V}_{\text{disease transmission}} - \underbrace{d_R I_R}_{\text{death}}$$

(1)

where the total adult female vector population density $N_V = S_V + I_V$, and the total reservoir population density $N_R = S_R + I_R$. See Table 2 for parameter definitions. At the disease-free equilibrium (DFE), the vector and reservoir population densities are denoted N_V^* and N_R^* respectively. In this model (eqn 1) we assume reservoir frequency-dependent disease transmission (after Anderson & May 1991); the choice of transmission terms is treated in the following section.

Table 2 Common notation for the arboviral encephalitis models reviewed here

Parameter	Symbol	Mean	Range	Sources* or equation
Vector				
Recruitment rate	a_V	–	–	–
Maturation rate	m_L	0.07	0.05–0.09	9, 12
Natural death rate, adults	d_V	0.03	0.02–0.07	13, 15, 20
Natural death rate, larvae	d_L	0.02	0.01–0.06	13, 15, 20
Birth rate assuming no larval class	b_V	Calc	Calc	$b_V = d_V$
Birth rate assuming larval class	b_L	Calc	Calc	$b_L = d_V(m_L + d_L)/m_L$
Infected proportion of births	ρ_V	0.001	0.000–0.002	1, 4, 7, 18
Probability of virus transmission to vector	α_V	0.69	0.23–1.00	2, 7, 14, 16, 17, 18, 21
Virus incubation rate	κ_V	0.10	0.09–0.12	14
Proportion surviving viral incubation period	φ_V	Calc	Calc	$\varphi_V = \kappa_V/(d_V + \kappa_V)$
Loss of infectivity	η_V	0.05	–	19
Biting rate	β_R	0.44	0.34–0.53	8
Biting rate per unit reservoir density	β'_R	Calc	Calc	$\beta'_R = \beta_R/\tilde{N}_R$ (see text)
Reservoirs				
Recruitment rate	a_R	–	–	–
Maturation rate	m_R	–	–	–
Natural death rate†	d_R	0.0015	0.001–0.002	3, 5, 10, 11
Birth rate $b_R = d_R$	b_R	Calc	Calc	–
Probability of virus transmission to reservoir	α_R	0.74	0.27–1.00	2, 6, 16, 17, 18, 19
Death rate from virus	δ_R	Calc	Calc	$\delta_R = \begin{cases} -\ln(\pi_R)/\tau_R & \text{for } \pi_R > 0 \\ 1/\tau_R & \text{for } \pi_R = 0 \end{cases}$
Recovery rate to immunity	γ_R	Calc	Calc	$\gamma_R = \begin{cases} -\ln(1 - \pi_R)/\sigma_R & \text{for } \pi_R < 1 \\ 1/\sigma_R & \text{for } \pi_R = 1 \end{cases}$
Loss of immunity rate	η_R	–	–	–

Subscript V refers to vectors, and R to reservoirs. All rates are per capita per day, except for the mosquito biting parameter for mass action β'_R, which is bites per day per unit density birds. Values indicated with – not used in $\mathcal{R}_0$ calculations. Species-specific values for three additional reservoir parameters, π_R, τ_R, and σ_R, shown in Table 3.

*Sources: 1, Bugbee & Forte (2004); 2, Colton *et al.* (2005); 3, Cornell Lab of Ornithology, http://www.birds.cornell.edu/; 4, Dohm *et al.* (2002); 5, Dyer *et al.* (1977); 6, Goddard *et al.* (2002); 7, Goddard *et al.* (2003); 8, Griffith & Turner (1996); 9, Hayes & Hsi (1975); 10, Hickey & Brittingham (1991); 11, Milby & Wright (1976); 12, Mpho *et al.* (2002); 13, Oda *et al.* (1999); 14, Sardelis & Turell (2001); 15, Suleman & Reisen (1979); 16, Tiawsirisup *et al.* (2004, 2005); 17, Turell *et al.* (2000); 18, Turell *et al.* (2001); 19, Vanlandingham *et al.* (2004); 20, Walter & Hacker (1974); 21, Work *et al.* (1955).

†Approximated from a range of rates reported for passerines.

TRANSMISSION TERMS

Disease transmission between vectors and reservoirs in arbovirus systems depends at its simplest on the mosquito biting rate. The term used to capture the biting rate in an *S–I* model may take one of several forms. We compare the assumptions and effects of three forms that have been used in these seven models: reservoir frequency dependence, mass action, and susceptible frequency dependence. The dynamics of reservoir frequency dependence can be thought of as intermediate between the extremes captured by the other two terms.

We will examine the biting rate from two perspectives: the number of bites per unit time by an individual vector, and the number of bites per unit time on an individual reservoir. We show how each transmission term is valid only within a range of vector and reservoir population densities, beyond which it

assumes an unrealistically high or low biting rate. We introduce notation for the vector and reservoir population densities at the DFE, at which the biting rates, and therefore the $\mathcal{R}_0$ values, coincide for the different transmission terms. Reservoir frequency dependence coincides with mass action at $\tilde{N}_R^*$ and $\tilde{N}_V^*$, the two forms of frequency dependence coincide at $\bar{N}_R^*$ and $\bar{N}_V^*$, and mass action coincides with susceptible frequency dependence at $\hat{N}_R^*$ and $\hat{N}_V^*$ (Fig. 2). The implications for the disease reproduction number, $\mathcal{R}_0$, are treated in the following sections.

Reservoir frequency dependence

The commonly used reservoir frequency-dependent transmission (eqn 1) follows Anderson & May (1991) in assuming that the vector biting rate is saturated, and not limited by reservoir density. In other words, the biting rate
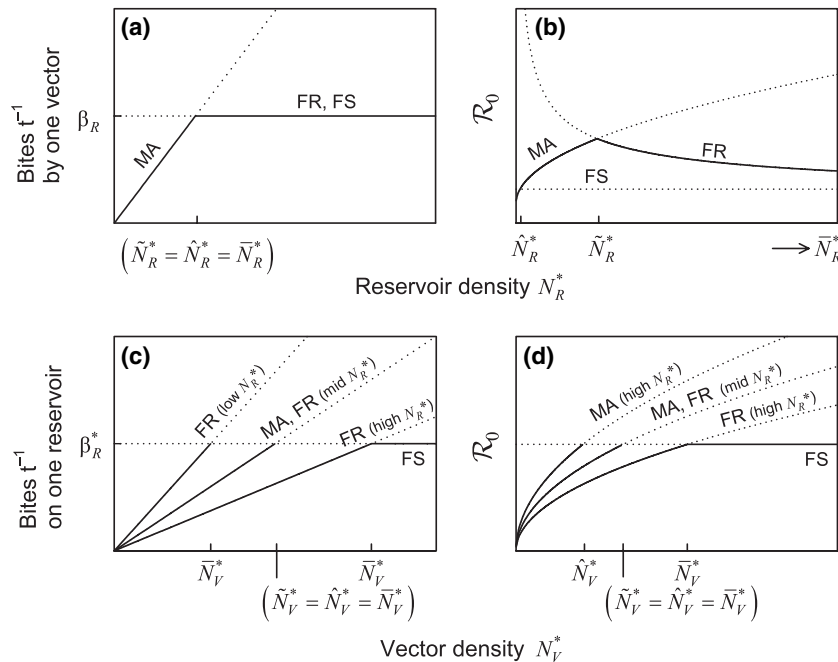
Figure 2 Different disease-transmission terms assume different biting rates (a,c) and lead to different reproduction numbers, $\mathcal{R}_0$ (b,d) in arboviral models. Each transmission term (FR, reservoir frequency dependence; MA, mass action; FS, susceptible frequency dependence) can appropriately be applied only at the population densities indicated by the solid lines. If a term is applied to populations in the dotted line regions, it will give misleadingly high or low $\mathcal{R}_0$ values. The number of bites per day by a single vector mosquito is shown as a function of reservoir density in (a), and the number of bites per day on a single reservoir is shown as a function of vector density in (c). The reproduction number $\mathcal{R}_0$ is shown as a function of reservoir density in (b) and vector density in (d). Threshold densities marked on the x-axes indicate intersection points for the three transmission terms. At mid-reservoir densities ($N_R^* = \tilde{N}_R^*$), the biting rates (a,c) and the $\mathcal{R}_0$ (b,d) of MA and FR coincide. At high reservoir densities ($N_R^* > \tilde{N}_R^*$), the biting rate on reservoirs for FR lies below that of MA, whereas at low reservoir densities ($N_R^* < \tilde{N}_R^*$), it lies above (c). At high reservoir densities, $\mathcal{R}_0$ for MA lies above that of FR (d); at low reservoir densities the relative positions of the two curves are swapped (not shown).

by vectors is constant across reservoir densities, and the biting rate experienced by reservoirs increases with vector density (Fig. 2a,c). Over the same range of vector densities, the biting rate on reservoirs increases faster for a lower reservoir density than for a higher one (Fig. 2c).

These biological assumptions are evident in the mathematical formulation of the transmission terms, in which the proportional susceptible and infectious reservoir densities appear (eqn 1). At the DFE, both populations are entirely susceptible, i.e. $S_R = N_R$ and $S_V = N_V$. Thus, at the DFE, the vector-to-reservoir transmission rate $\beta_R I_V S_R / N_R$ depends only on the vector biting rate, while the reservoir-to-vector transmission rate $\beta_R S_V I_R / N_R$ depends also on the ratio of vector and reservoir densities (eqn 1).

Under reservoir frequency dependence, the biting rate by vector mosquitoes is taken to be the maximal rate allowed by the gonotrophic cycle, i.e. the minimum time required between blood meals for a female to produce and lay eggs. This biting rate, β_R, has units per time, and can be thought of as the maximum possible number of bites per day made

by a single mosquito. In contrast, the biting parameter for mass-action transmission has different dimensions. (See Begon *et al.* 2002 for further explanation of transmission term units.) Reservoir frequency dependence is used in models WN1, WN3, WN4 and WN5.

Mass action

A second common disease transmission term is mass action (e.g. McCallum *et al.* 2001). Mass action assumes that biting rates are limited by the densities of both vectors and reservoirs (Fig. 2a,c). At the DFE, the vector-to-reservoir transmission rate $\beta_R' I_V S_R$ is thus a function of reservoir density, whereas the reservoir-to-vector transmission rate $\beta_R' S_V I_R$ is a function of vector density (Fig. 2a,c).

Although the assumption of mass action is widely used, it is valid only up to the threshold reservoir density denoted $\tilde{N}_R^*$. We can understand this limit by examining the transmission term, in which the biting parameter β_R' has units per time per density, and can be thought of as the number of bites per day made by a single vector, per unit

density of reservoirs. It is calculated as $\beta'_R = \beta_R / \tilde{N}^*_R$. Above $\tilde{N}^*_R$, the vector biting rate in units of bites per time, $\beta'_R N^*_R$, would exceed β_R, and therefore by definition would exceed the physiological capacity of the vector (Fig. 2a). The vector biting rates under mass action and reservoir frequency dependence coincide when $N^*_R = \tilde{N}^*_R$ (Fig. 2a). At lower reservoir densities where $N^*_R < \tilde{N}^*_R$, the biting rate of reservoir frequency dependence is unrealistically high. At higher densities where $N^*_R > \tilde{N}^*_R$, the biting rate of mass action is unrealistically high. Mass action is used in models WN2 and RR.

Susceptible frequency dependence

A third type of transmission, susceptible frequency dependence, assumes that the biting rate is not limited by either reservoir or vector density. The resulting vector biting rate β_R is the same as for reservoir frequency dependence (Fig. 2a). However, the biting rate on reservoirs is assumed to be at some maximum, denoted β^*_R, which is reached at a threshold vector density (Fig. 2c). Even if the vector density exceeds this threshold, the biting rate experienced by reservoirs does not exceed β^*_R. We consider this latter assumption unlikely to hold in an ecological system. However, as it is used in model JE and subsequent analyses (Tapaswi et al. 1995, Ghosh & Tapaswi 1999), we examine its structure and implications.

Mathematically, the transmission terms for susceptible frequency dependence are formulated as a function of the proportional susceptible population, whether reservoir or vector. The vector-to-reservoir term, $\beta_R I_V S_R / N_R$, is the same as for reservoir frequency dependence, but the reservoir-to-vector term $\beta_R I_R S_V / N_V$ is not. Under susceptible frequency dependence, the vector biting rate β_R intersects that of mass action at $\hat{N}^*_R$ (Fig. 2a). The biting rate on reservoirs, β^*_R, intersects that of mass action at the threshold vector density $\hat{N}^*_V$, and that of reservoir frequency dependence at $\bar{N}^*_V$ (Fig. 2c). Susceptible frequency dependence would clearly overestimate the biting rates below these threshold population densities (Fig. 2a,c). In the absence of empirical evidence for a vector-density threshold, this is probably not a biologically applicable transmission term.

Each model in this review uses one of these three transmission terms (Table 1). More complex models could incorporate saturating or other transmission functions to capture a range of spatial and temporal variation in host and vector population densities (e.g. McCallum et al. 2001; Keeling 2005).

EFFECT OF TRANSMISSION TERMS ON $\mathcal{R}_0$

The disease basic reproduction number, $\mathcal{R}_0$, provides key insights into disease outbreak and control (Anderson &

May 1991; Hethcote 2000; Dobson & Foufopoulos 2001; Heesterbeek 2002; Heffernan et al. 2005). It represents the average number of secondary infections deriving from the introduction of an infected individual into an otherwise susceptible population. Quantitatively, it has a threshold value of 1: when $\mathcal{R}_0 > 1$ a disease outbreak can occur, and when $\mathcal{R}_0 < 1$ it will not. Qualitatively, the expression for $\mathcal{R}_0$ indicates which elements of the disease system can be manipulated to reduce the chance of an outbreak.

To evaluate the effects of different model features on $\mathcal{R}_0$, we first determine analytical expressions for $\mathcal{R}_0$ using the next generation matrix method (Diekmann & Heesterbeek 2000; van den Driessche & Watmough 2002). For details, see the Appendix. The three disease-transmission terms, reservoir frequency dependence, mass action and susceptible frequency dependence, generate different expressions for $\mathcal{R}_0$, with different implications for disease outbreak prediction and control (Fig. 2c,d).

Reservoir frequency dependence

The core model with reservoir frequency-dependent transmission (eqn 1; Fig. 1a) has the basic reproduction number

$$R_0 = \sqrt{\underbrace{\frac{\beta_R}{d_V}}_{\text{vector to reservoir}} \underbrace{\frac{\beta_R N^*_V}{d_R N^*_R}}_{\text{reservoir to vector}}} \quad . \qquad (2)$$

This expression consists of two elements under the square root sign. The first represents the number of secondary reservoir infections caused by one infected vector. The second represents the number of secondary vector infections caused by one infected reservoir. Taking the square root gives the geometric mean of these two terms, which can be interpreted as $\mathcal{R}_0$ for the addition of an average infected individual, whether vector or reservoir, to an otherwise susceptible system.

This $\mathcal{R}_0$ expression (eqn 2) with frequency-dependent transmission is notable in that it contains the ratio of the susceptible vector and reservoir densities at the DFE. By inspection, we can see that reducing the vector density N^*_V will reduce $\mathcal{R}_0$ and therefore help prevent an outbreak (Fig. 2d). In contrast, reducing the reservoir density N^*_R will increase $\mathcal{R}_0$ and therefore increase the chance of outbreak (Fig. 2b). Although this latter result may seem initially counterintuitive, it follows directly from the biological assumption that the vector biting rate is not affected by reservoir density (Fig. 2a). Consequently, a reduction in reservoir density means the remaining individuals are bitten more frequently. This focuses disease transmission on a few highly bitten individuals that are more likely to become infected and more likely to re-infect the vectors. Setting

$\mathcal{R}_0 = 1$ under reservoir frequency dependence gives the threshold vector density for a disease outbreak, $N_{VT}^* = d_V d_R N_R^*/\beta_R^2$, which is an increasing function of reservoir density.

Mass action

Using mass-action transmission in the core model gives a different reproduction number, namely

$$R_0 = \sqrt{\frac{\beta_R'}{d_V}\frac{\beta_R' N_V^* N_R^*}{d_R}}. \tag{3}$$

In this case, $\mathcal{R}_0$ is sensitive not to the ratio, but to the absolute densities of vectors and hosts. Thus, the model predicts that reducing either vector or reservoir density will reduce $\mathcal{R}_0$ and reduce the chance of disease outbreak (Fig. 2b,d). In terms of the reservoir population, this prediction is opposite to that of reservoir frequency dependence.

The $\mathcal{R}_0$ for mass action and reservoir frequency dependence are equal when the reservoir density $N_R^* = \tilde{N}_R$ (Fig. 2b,d). The consequence of misapplying mass action at higher reservoir density is that $\mathcal{R}_0$ is artificially high (Fig. 2b). In contrast, the $\mathcal{R}_0$ of reservoir frequency dependence is artificially high at lower reservoir density (Fig. 2b). With respect to vector density, the $\mathcal{R}_0$ curves for both transmission terms overlap when $N_R^* = \tilde{N}_R$ (Fig. 2d). When $N_R^* > \tilde{N}_R$, the curve for mass action is higher and that for reservoir frequency dependence is lower (Fig. 2d). In the opposite case of $N_R^* < \tilde{N}_R$, the relative positions of the two curves are reversed.

Setting $\mathcal{R}_0 = 1$ under mass action gives the threshold vector density $N_{VT}^* = d_V d_R/\beta_R'^2 N_R^*$, which is a decreasing function of reservoir density. This threshold for vector–host models can be compared with that resulting from mass-action transmission in directly transmitted disease models (McCallum *et al.* 2001).

Susceptible frequency dependence

When disease transmission is assumed to be susceptible frequency dependent, the vector and host densities cancel out during the calculation of $\mathcal{R}_0$. The resulting reproduction number is a constant value that does not vary with the density of either species,

$$R_0 = \sqrt{\frac{\beta_R}{d_V}\frac{\beta_R}{d_R}}. \tag{4}$$

This formulation differs importantly from the previous two, in that it predicts that the chance of disease outbreak is not influenced by controlling either reservoir or vector densities (Fig. 2b,d). The lack of density threshold for disease outbreak in susceptible frequency-dependent trans-

mission can be compared with the case for frequency dependence in a directly transmitted disease model (McCallum *et al.* 2001).

With respect to the reservoir density, $\mathcal{R}_0$ for susceptible frequency dependence intersects that of mass action at $\hat{N}_R^*$ (Fig. 2b), which is also when the densities $N_V^* N_R^* = 1$ (compare eqns 3 and 4). The $\mathcal{R}_0$ values for the two frequency-dependent terms intersect at $\bar{N}_R^*$ (Fig. 2b), which is also when the densities $N_V^*/N_R^* = 1$ (compare eqns 2 and 4). With respect to vector density, $\mathcal{R}_0$ for susceptible frequency dependence intersects that of mass action at $\hat{N}_V^*$, and that of reservoir frequency dependence at $\bar{N}_V^*$ (Fig. 2c). When $N_R^* = \tilde{N}_R^*$, the vector density thresholds coincide for all three transmission terms (Fig. 2d).

If the assumptions of susceptible frequency dependence held in a natural system, mass action and reservoir frequency dependence would give an artificially high $\mathcal{R}_0$ if misapplied above the threshold vector density (Fig. 2d). However, since these assumptions seem unlikely to hold, we anticipate that susceptible frequency dependence will almost always give an incorrect $\mathcal{R}_0$.

The appropriate choice of disease-transmission term is clearly determined by the vector and host population densities. For a given vector density, it is appropriate to assume mass-action transmission when low reservoir densities limit the biting rate, and reservoir frequency dependence at higher reservoir densities where the biting rate is saturated (Fig. 2a). For a given reservoir density, it seems appropriate to assume mass action or reservoir frequency dependence across all vector densities (Fig. 2c). Choosing an inappropriate transmission term can lead to a misleadingly high or low $\mathcal{R}_0$, and correspondingly inaccurate disease predictions (Fig. 2b,d).

Numerical values of $\mathcal{R}_0$

The qualitative analysis above illustrates how different transmission terms alter the expressions and interpretations of $\mathcal{R}_0$. Do these results translate into significant differences in the numerical estimates of $\mathcal{R}_0$? To address this question, we generate quantitative $\mathcal{R}_0$ estimates that incorporate the underlying variation in the constituent model parameters. We follow a standard methodology of constructing a triangular distribution for each parameter, based on reported minimum, mean and maximum estimates. We then use 10 000 Monte Carlo realizations from each triangular distribution to generate an estimated distribution of $\mathcal{R}_0$ (e.g. Blower & Dowlatabadi 1994; Sanchez & Blower 1997; Chowell *et al.* 2004). Distributions that do not overlap at the fifth or 95th percentiles are taken to be significantly different.

For parameter estimates from a single study, we used the minimum, mean, and maximum values reported in that study. When more than one study was available, we took the

overall mean of the average values across studies, and the minimum and maximum from all studies combined (Tables 2 and 3). For parameters with only a single point estimate, we used that value as a constant. The reported values for most parameters were based on small sample sizes, so we consider the estimates and distributions used here to be preliminary.

For vectors, we preferentially used parameter values from the mosquitoes *Culex pipiens* sspp., and used related species (*Culex quinquefasciatus* and *Culex tritaeniorhynchus*) when necessary. Most reservoir data, including virus transfer estimates between vectors and reservoirs, were based on experiments with domestic chickens (*Gallus gallus*), but in some cases multiple species were used. To compare $\mathcal{R}_0$ for different model structures, we used mortality and recovery rates for house sparrows *Passer domesticus*. We later compare a single model using mortality and recovery rates for six North American reservoir species.

Different transmission functions in the core model led to significantly different numerical estimates of $\mathcal{R}_0$, ranging over an order of magnitude or more (Fig. 3). At low reservoir density where mass action applies, the $\mathcal{R}_0$ of reservoir frequency dependence was significantly higher, and that of susceptible frequency dependence significantly lower (Fig. 3a). At the threshold reservoir density where both mass action and reservoir frequency dependence apply, the $\mathcal{R}_0$ of susceptible frequency dependence remained significantly lower. At higher reservoir density where only reservoir frequency dependence applies, the $\mathcal{R}_0$ of mass action was significantly higher, and that of susceptible frequency dependence significantly lower (Fig. 3a).

At lower vector densities where mass action and reservoir frequency dependence apply, the $\mathcal{R}_0$ of susceptible frequency dependence tended to be higher (Fig. 3b). At the intermediate threshold vector density where all three transmission terms are equivalent, the $\mathcal{R}_0$ distributions

Table 3 Mean (and range) of infection and mortality parameter values for six West Nile virus bird reservoir species

Parameter	Probability of surviving infection	Days infectious	Days to death
Symbol	π_R	σ_R	τ_R
American crow	0.00	3.25 (3–5)	5.1 (4–6)
American robin	1.00	3 (4–5)	n.a.
Blue jay	0.25	3.75 (3–5)	4.7 (4–5)
House sparrow	0.47 (0.16–0.90)	3 (2–6)	4.7 (3–6)
Northern mockingbird	1.00	1.25 (1–2)*	n.a.
Northern cardinal	0.78	1.5 (1–3)*	4

Sources: Komar *et al.* (2003, 2005); Brault *et al.* (2004); Langevin *et al.* 2005; Reisen *et al.* 2005; Work et al. (1955).
*Mean and maximum values from Komar *et al.* (2005); minimum value of 1 day selected for simulation purposes.
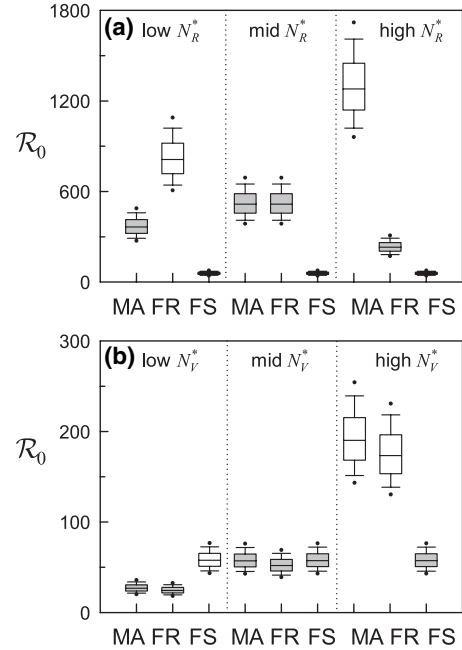
Figure 3 Numerical estimates of $\mathcal{R}_0$ differ significantly for the core arboviral model under three different transmission assumptions: MA, mass action; FR, reservoir frequency dependence; FS, susceptible frequency dependence. Vertical dotted lines separate regions of low $(N_R^* < \tilde{N}_R^*)$, medium $(N_R^* = \tilde{N}_R^*)$, and high $(N_R^* > \hat{N}_R^*)$ reservoir densities in (a) and low $(N_V^* < \hat{N}_V^*)$, medium $(N_V^* = \tilde{N}_V^*)$, and high $(N_V^* > \bar{N}_V^*)$ vector densities in (b). Shaded boxes indicate the biologically appropriate transmission terms for each population density range (all FS boxes in (a) are unshaded). Sample population densities chosen to illustrate different regions of $\mathcal{R}_0$ curves, expressed as number km^{-2}, are (a) $N_V^* = 1000, \tilde{N}_R^* = 100$, and $N_R^* = 50$ (low), 100 (mid), and 500 (high), and (b) $\tilde{N}_R^* = 500, N_R^* =, 550$, and $N_V^* = 100$ (low), 450 (mid), and 5000 (high). Parameter values as in Tables 2 and 3, using disease mortality and recovery rates for house sparrows. Boxes show median and 25th and 75th percentiles, bars show 10th and 90th percentiles, and dots show fifth and 95th percentiles.

overlapped substantially. In the hypothetical case of susceptible frequency dependence, the $\mathcal{R}_0$ of mass action and reservoir frequency dependence were significantly higher when $N_V^* > \tilde{N}_V^*$ (Fig. 3b). These numerical results show that, for these parameter values, a transmission term applied to an inappropriate host or vector population density can over- or underestimate $\mathcal{R}_0$ by an order of magnitude or more.

EFFECTS OF OTHER MODEL FEATURES

We now return to the core model (eqn 1) and investigate the effects on $\mathcal{R}_0$ of different epidemiological features, species parameter values and life history features.

Epidemiological features

The seven arboviral models include a range of epidemiological parameters (Table 1, Fig. 1b). For vectors, some models add an exposed class (E_V) with an associated transition rate to account for the observed viral incubation period in mosquitoes. Additional vector modifications include a return rate from infectious to susceptible, and a vertical (transovarial) transmission probability from infected vectors E_V and I_V to their offspring (Table 1, Fig. 1b).

For reservoirs, most models add a recovered reservoir class (R_R), which allows immune reservoirs to remain in the disease system. Most models also incorporate disease-induced mortality in infectious individuals, and one adds loss of immunity in recovered individuals (Table 1, Fig. 1b). Horizontal transmission among reservoir hosts has been reported empirically (Kuno 2001), but its scale and importance remain to be determined and we have not yet seen it incorporated in a published model. The above epidemiological features can be added to the core model by using the following system of ordinary differential equations:

$$\frac{dS_V}{dt} = \underbrace{b_V[S_V + (1-\rho_V)(E_V + I_V)]}_{\text{birth of susceptibles}}$$

$$\underbrace{-\ \alpha_V \beta_R \frac{I_R}{N_R} S_V}_{\text{disease transmission}} + \underbrace{\eta_V I_V}_{\text{loss of infectivity}} \underbrace{-\ d_V S_V}_{\text{death}}$$

$$\frac{dE_V}{dt} = \underbrace{b_V \rho_V (E_V + I_V)}_{\text{birth of infecteds}} + \underbrace{\alpha_V \beta_R \frac{I_R}{N_R} S_V}_{\text{disease transmission}}$$

$$\underbrace{-\ (d_V + \kappa_V)E_V}_{\text{death and incubation}}$$

$$\frac{dI_V}{dt} = \underbrace{\kappa_V E_V}_{\text{incubation}} - \underbrace{(d_V + \eta_V)I_V}_{\text{death and loss of infectivity}}$$

$$\frac{dS_R}{dt} = - \underbrace{\alpha_R \beta_R \frac{S_R}{N_R} I_V}_{\text{disease transmission}} - \underbrace{d_R S_R}_{\text{death}} + \underbrace{\eta_R R_R}_{\text{loss of immunity}}$$

$$\frac{dI_R}{dt} = \underbrace{\alpha_R \beta_R \frac{S_R}{N_R} I_V}_{\text{disease transmission}} - \underbrace{(d_R + \delta_R + \gamma_R)I_R}_{\text{death, disease mortality and recovery}}$$

$$\frac{dR_R}{dt} = \underbrace{\gamma_R I_R}_{\text{recovery}} - \underbrace{(d_R + \eta_R)R_R}_{\text{death and loss of immunity}} .$$

(5)

This expanded model (eqn 5) incorporates the exposed vector class as in models WN1, WN2, WN3 and RR, vector vertical transmission as in WN2 and WN5, reservoir disease mortality as in WN1, WN3, WN4 and WN5, reservoir recovery as in all but WN4, and reservoir loss of immunity and vector loss of infectivity as in JE.

The basic reproduction number for this model, in the absence of vector vertical disease transmission, is

$$R_0 = \sqrt{\frac{\varphi_V \alpha_R \beta_R}{(d_V + \eta_V)} \frac{\alpha_V \beta_R N_V^*}{(d_R + \delta_R + \gamma_R)N_R^*}}.$$

(6)

With vertical disease transmission, i.e. with $\rho_V > 0$,

$$R_0 = \frac{c_V \rho_V}{2} + \sqrt{\left(\frac{c_V \rho_V}{2}\right)^2 + \frac{\varphi_V \alpha_R \beta_R}{(d_V + \eta_V)} \frac{\alpha_V \beta_R N_V^*}{(d_R + \delta_R + \gamma_R)N_R^*}},$$

(7)

where

$$c_V = b_V \left(\frac{\varphi_V}{(d_V + \eta_V)} + \frac{1}{(d_V + \kappa_V)} \right).$$

(8)

As $\mathcal{R}_0$ is a disease outbreak threshold, we can assess the role of each model element in eqn 7 in contributing to the chance of an outbreak. Only the probability of vertical transmission from female vectors to their offspring, $\rho_V > 0$, increases $\mathcal{R}_0$. All the other epidemiological features decrease $\mathcal{R}_0$. The exposed vector compartment reduces $\mathcal{R}_0$ by introducing into the numerator the proportion of vectors surviving the viral incubation period to become infectious (φ_V). The virus transmission probabilities in the numerator (α_V, α_R), and the added vector and reservoir loss rates in the denominator (η_V, δ_R, γ_R), also reduce $\mathcal{R}_0$.

An additional term that might intuitively be expected to increase the chance of disease outbreak is reservoir loss of immunity, η_R. However, this term does not appear in $\mathcal{R}_0$. Its absence results from the definition of $\mathcal{R}_0$, which is calculated at the DFE using only the equations for infected individuals, and is valid only during the earliest stages of an outbreak. Terms such as η_R that do not appear in the equations for infected individuals will not appear in $\mathcal{R}_0$, although they may still influence the predicted long-term disease trajectory.

These different epidemiological features also affect the numerical estimate of $\mathcal{R}_0$. For the sample parameter values used here, $\mathcal{R}_0$ values ranged over two orders of magnitude (Fig. 4a). The two parameters with the greatest individual influence on $\mathcal{R}_0$ were the added reservoir loss terms: the disease-induced death rate δ_R and the recovery rate γ_R (Fig. 4a). Both rates are two to three orders of magnitude greater than the natural death rate d_R (Table 3). Among the seven arboviral models, these three loss rates are incorporated in different combinations: two models use all three terms, but the others use subsets $(d_R + \delta_R)$, $(d_R + \gamma_R)$, $(\delta_R + \gamma_R)$, and γ_R alone (Table 1). For the sample parameter values used
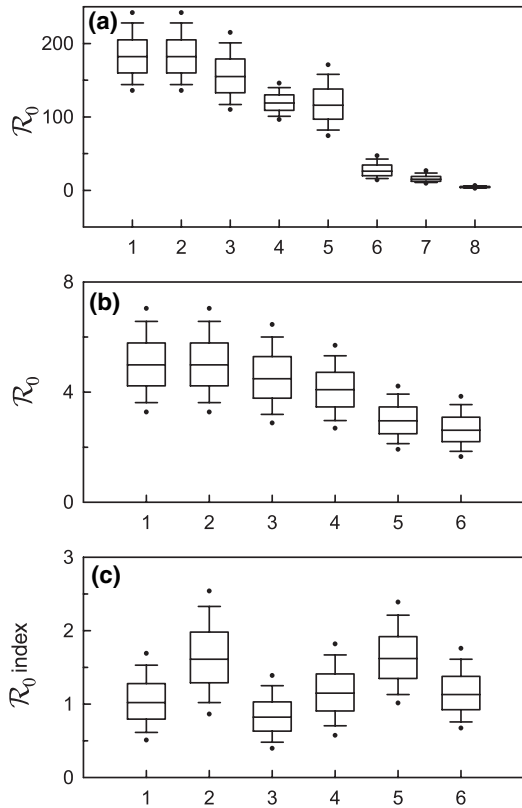
Figure 4 The reproduction number $\mathcal{R}_0$ differs for different epidemiological features added to the arboviral core model (a), and for different reservoir bird species (b,c). In (a), $\mathcal{R}_0$ shown for (1) the core model, and the core model with added parameters; (2) ρ_V; (3) φ_V; (4) η_V; (5) α_V and α_R; (6) γ_R; (7) δ_R; (8) the core model with all additional parameters. Parameter values as in Tables 2 and 3, using disease mortality and recovery rates for house sparrows. In (b), $\mathcal{R}_0$ as in eqn 6 shown for different reservoir bird species: (1) American crows; (2) American robins; (3) house sparrows; (4) blue jays; (5) Northern mockingbirds; (6) Northern cardinals. In (c) the $\mathcal{R}_0$ index indicates relative reservoir capacity of the same species, accounting for their relative abundances and vector feeding preferences. Parameter values as in Tables 2 and 3; population densities $(N_V^*, N_R^*) = (10\,000\ \mathrm{km}^{-2},\ 1000\ \mathrm{km}^{-2})$. Boxes show median and 25th and 75th percentiles, bars show 10th and 90th percentiles, and dots show fifth and 95th percentiles.

here, the choice of loss terms clearly has a significant effect on a model's $\mathcal{R}_0$. The individual addition of the remaining five epidemiological parameters generated $\mathcal{R}_0$ distributions overlapping that of the core model (Fig. 4a). The model with all features combined had the lowest $\mathcal{R}_0$ (Fig. 4a).

Variation among reservoir species

The quantitative effects of adding these different epidemiological features depend to some extent on the species chosen for model parameterization. We illustrate this effect

by estimating $\mathcal{R}_0$ values for six common North American bird species, American crows *Corvus brachyrhynchos*, American robins *Turdus migratorius*, blue jays *Cyanocitta cristata*, house sparrows *Passer domesticus*, Northern mockingbirds *Mimus polyglottos* and Northern cardinals *Cardinalis cardinalis*. We first estimate $\mathcal{R}_0$ assuming each species constitutes simultaneously the entire blood meal source population for mosquitoes, and the entire disease reservoir population (Fig. 4b). We then estimate a more ecologically informative $\mathcal{R}_0$ index that assumes all species are available for blood meals, but only one species can act as a disease reservoir (Fig. 4c).

For each bird, we used species-specific values of δ_R and γ_R (Table 3). An additional species-specific parameter reported in the empirical literature is the mean infectiousness rate, i (Komar *et al.* 2003), which would correspond to the transition rate from exposed to infectious classes if reservoirs were modelled with an *S–E–I–R* structure. As this approach has not yet been taken in these models, we did not incorporate it here. The resulting $\mathcal{R}_0$ distributions for the six species are all significantly above the threshold value of 1, illustrating that each species could serve as a reservoir for a West Nile virus outbreak (Fig. 4b). Under the assumption that each bird species was the only mosquito blood meal source, the $\mathcal{R}_0$ for American crows is highest, and that of Northern cardinals the lowest.

Realistically, of course, multiple reservoir species are simultaneously present, and the biting rates they experience vary according to their abundance and to vector preference. When this is taken into consideration, the reservoir species' relative contributions to disease outbreak alter. We explore these factors by introducing an $\mathcal{R}_0$ index to give a relative ranking for each reservoir species that incorporates its contribution to the proportion of mosquito blood meals in a natural system. To do this, we multiply the mosquito biting rate by the reported proportion of blood meals for each species, and calculate $\mathcal{R}_0$ according to the same formula as above. The resulting $\mathcal{R}_0$ index values will always be lower than the true $\mathcal{R}_0$ for each species, and cannot be used to predict a disease outbreak. They do, however, allow a relative rank comparison of reservoir species in a fuller ecological context.

In this example, we constructed triangular parameter distributions based on the mean and approximate range of *Cx. pipiens* spp. blood meal proportions reported for the same six bird species in one study in Tennessee: crows 2.8%, 0–8.2%; robins 11.1%, 0.8–21.4%, jays 8.3%, 0–17.3%; sparrows 2.8%, 0–8.2%; mockingbirds 30.6%, 15.6–45.6%; cardinals 19.4%, 6.5–32.3% (Apperson *et al.* 2004). We then multiplied the biting rate by this proportion, and calculated $\mathcal{R}_0$ as before. We emphasize that since these blood meal data are drawn only from a single case study, the index values calculated here are specific to this Tennessee season and locale.

The $\mathcal{R}_0$ index distributions indicate that the six reservoir species are comparable in their potential contribution to a disease outbreak (Fig. 4c). The difference between species ranks in Fig 4a,b arises because species with a higher $\mathcal{R}_0$ in Fig. 4b had a lower proportion of blood meals (e.g. crows) and those with a lower $\mathcal{R}_0$ in Fig. 4b had a higher proportion of blood meals (e.g. cardinals). The advantage of using this $\mathcal{R}_0$ index is that it incorporates both disease transmission and blood meal data, providing a more realistic assessment of the relative role each reservoir species would be likely to play in a natural disease outbreak.

Life history features

We return again to the core arboviral model to consider the effects of adding vital dynamics and stage structure on $\mathcal{R}_0$ (Table 1, Fig. 1c). The vital rates for vector mosquitoes, which have a relatively short lifecycle on the order of 1 month, are already incorporated in the core model. More complex seasonal or density-dependent recruitment functions can also be used (e.g. WN1 and JE) but limit the model's analytical tractability. Larval and pupal stages, which may represent up to a quarter of the vector lifespan, but are not involved in vector–host disease transmission, may be added as an additional class (as in WN3).

For reservoirs, a birth rate must be considered if the model is to apply beyond a single season. Again, this may be added as a constant term or as a more complex function. Reservoir stage structure can be used to account for different disease susceptibilities of, for example, juveniles and adults (e.g. WN1). The core model can be modified to include these vital dynamics and stage structures as follows (Fig. 1c):

$$\underbrace{\frac{\mathrm{d}L_V}{\mathrm{d}t}}_{\text{Larval vectors}} = \underbrace{b_L N_V}_{\text{birth}} - \underbrace{(d_L + m_L)L_V}_{\text{death and maturation}}$$

$$\underbrace{\frac{\mathrm{d}S_V}{\mathrm{d}t}}_{\text{Susceptible vectors}} = \underbrace{m_L L_V}_{\text{maturation}} - \underbrace{\alpha_V\left(\beta_r\frac{I_r}{N_r} + \beta_R\frac{I_R}{N_R}\right)S_V}_{\text{disease transmission}}$$
$$- \underbrace{d_V S_V}_{\text{death}}$$

$$\underbrace{\frac{\mathrm{d}I_V}{\mathrm{d}t}}_{\text{Infectious vectors}} = \underbrace{\alpha_V\left(\beta_r\frac{I_r}{N_r} + \beta_R\frac{I_R}{N_R}\right)S_V}_{\text{disease transmission}} - \underbrace{d_V I_V}_{\text{death}}$$

$$\underbrace{\frac{\mathrm{d}S_r}{\mathrm{d}t}}_{\text{Susceptible juvenile reservoirs}} = \underbrace{b_r N_R}_{\text{birth}} - \underbrace{\alpha_r\beta_r\frac{S_r}{N_r}I_V}_{\text{disease transmission}}$$
$$- \underbrace{(d_r + m_r)S_r}_{\text{death and maturation}}$$

$$\underbrace{\frac{\mathrm{d}S_R}{\mathrm{d}t}}_{\text{Susceptible adult reservoirs}} = \underbrace{m_r S_r}_{\text{maturation}} - \underbrace{\alpha_R\beta_R\frac{S_R}{N_R}I_V}_{\text{disease transmission}} - \underbrace{d_R S_R}_{\text{death}}$$

$$\underbrace{\frac{\mathrm{d}I_i}{\mathrm{d}t}}_{\text{Infectious reservoirs}} = \underbrace{\alpha_i\beta_i\frac{S_i}{N_i}I_V}_{\text{disease transmission}}$$
$$- \underbrace{(d_i + \delta_i + \gamma_i)I_i}_{\text{death, disease mortality and recovery}} \quad, \quad i = r, R$$

$$\underbrace{\frac{\mathrm{d}R_R}{\mathrm{d}t}}_{\text{Recovered reservoirs}} = \underbrace{\gamma_r I_r + \gamma_R I_R}_{\text{recovery}} - \underbrace{d_R R_R}_{\text{death}}$$

$$(9)$$

This model (eqn 9) incorporates a vector larval stage L_V with associated birth rate b_L and maturation rate m_L, as in WN3. It also includes a simplified reservoir stage structure based on WN1, where the population is divided into younger and older stages denoted with subscripts r and R respectively. Equation 9 also includes parameters from eqn 5 that may differ between the two reservoir stages (α_i, β_i, d_i, δ_i, γ_i; $i = r, R$), and includes the parameter α_V for symmetry in disease transmission. It has the basic reproduction number

$$R_0 = \sqrt{\frac{\alpha_V N_V^*}{d_V}\left(\frac{\alpha_r\beta_r^2}{(d_r + \delta_r + \gamma_r)N_r^*} + \frac{\alpha_R\beta_R^2}{(d_R + \delta_R + \gamma_R)N_R^*}\right)}.$$

$$(10)$$

To evaluate the effects of these life history features on $\mathcal{R}_0$, we follow model WN1 in assuming that juvenile reservoirs are more susceptible than adults to both natural and disease mortality, and recover more slowly from infection. Relative to a homogeneous adult population, the additional terms $d_r > d_R$ and $\delta_r > \delta_R$ therefore decrease $\mathcal{R}_0$, whereas $\alpha_r > \alpha_R$ and $\gamma_r < \gamma_R$ increase $\mathcal{R}_0$. The net effect of adding a juvenile stage thus depends on the differences in parameter values and on the relative densities of the two stages (see for example Lord & Day 2001a,b). The addition of vector-stage structure does not influence $\mathcal{R}_0$ or the disease trajectory. This is because of the steady-state assumption at the DFE that $b_L = d_V(m_L + d_L)/m_L$ (Wonham *et al.* 2004), which means that vector replacement in the population is instantaneous.

Incorporating two or more reservoir species (e.g. Dobson 2004) or vector species (e.g. Choi *et al.* 2002) would similarly introduce additional equations and parameter sets into $\mathcal{R}_0$. The net effect of these additions, in terms of disease dilution or amplification (Dobson 2004), would again depend on the relative densities of each species and on the specific parameter values.

IMPLICATIONS AND FUTURE DIRECTIONS

Implications of model comparison

In this review, we have synthesized a group of mathematical models to illustrate how biological assumptions alter model predictions in host–vector diseases. Our analytical results show that different disease-transmission assumptions generate fundamentally different disease basic reproduction numbers. The qualitative differences in $\mathcal{R}_0$ expressions can lead to diametrically opposed predictions for disease control, and the quantitative $\mathcal{R}_0$ values can span orders of magnitude. These conflicting predictions can be reconciled by appreciating that each disease-transmission term can realistically be applied only to a certain range of vector and reservoir population densities. If a term is misapplied outside this range, the resulting $\mathcal{R}_0$ values can be misleadingly low or high, and predicted control strategies may backfire.

The assumption of reservoir frequency-dependent transmission applies when the biting rate by vectors is saturated but the biting rate on reservoirs is not. It predicts that controlling the vector density decreases the chance of disease outbreak, whereas controlling the reservoir density increases the chance of outbreak. This is in stark contrast to the other transmission terms. Mass-action transmission, which applies when both biting rates are limited by low vector and reservoir densities, predicts that controlling either vector or host density will reduce the chance of disease outbreak. Susceptible frequency dependence, which assumes that the biting rates by vectors and on reservoirs are both saturated, predicts that control of neither vector nor host density will influence the chance of disease outbreak, but this assumption seems unlikely to hold in a natural system. Quantitatively, the use of an inappropriate transmission term can incorrectly increase or decrease the estimate of $\mathcal{R}_0$ by a factor of two or more orders of magnitude in the examples we calculated. As each of the three transmission terms is in use in West Nile virus and related disease modelling (Table 1), it is essential to establish which is appropriate for a given system before making model-based disease predictions and control recommendations.

Additional assumptions about disease epidemiology also significantly affected $\mathcal{R}_0$. For the system we examined, simpler models with fewer parameters generated higher $\mathcal{R}_0$ values, and therefore a greater predicted risk of outbreak, than more complex and realistic models. The $\mathcal{R}_0$ of the most complex model was some two orders of magnitude lower than that of the simplest model.

Comparing the $\mathcal{R}_0$ of six bird species showed that all are intrinsically effective reservoirs for a West Nile virus outbreak, with American crows the highest and Northern cardinals the lowest. We introduced the $\mathcal{R}_0$ index to identify the relative contributions of each species in an ecological context that includes the proportion of mosquito blood meals that each species supplies. The $\mathcal{R}_0$ index values for all six species were indistinguishable, showing that all could play an approximately equal role in an outbreak.

For clarity, we separately synthesized the effects of transmission terms, epidemiological features, and life history features, but for a given model the effects of all these assumptions should be assessed together. Most of the seven original arboviral encephalitis models presented numerical simulations of the disease trajectory, but in only one case were these validated against observed outbreak data (WN3). With the seven models now synthesized into a systematic array, reasonable next steps would include model parameterization, validation against independent data, and model selection. As most of the parameter estimates for West Nile virus are currently based on small sample sizes, parameterization would be more robust with more accurate and precise distributions for all relevant species. Validation against outbreak data would be enhanced by field estimates of these same vector and reservoir species' densities at the beginning of the outbreak. With the resulting parameter estimates and quantified uncertainty in hand, appropriate transmission terms could better be selected, the models could better be tested and compared, and the sensitivity of $\mathcal{R}_0$ more accurately assessed.

Future directions in arboviral encephalitis modelling

The model variations that we synthesized here are sufficiently simple to remain analytically tractable. However, important extensions in environmental, ecological, and evolutionary model complexity could also be developed and tested for host–vector models in general, and for West Nile virus in particular.

Extrinsic environmental factors influence seasonal and interannual population dynamics of both vectors and hosts (Shaman *et al.* 2002; Hosseini *et al.* 2004; Pascual & Dobson 2005) and could be incorporated into the model structure both analytically and numerically (e.g. Lord & Day 2001a,b; Koelle & Pascual 2004; Wonham *et al.* 2004). Spatial models (e.g. Hastings *et al.* 2005; Lewis *et al.* 2006a) could incorporate both environmental variability and animal dispersal patterns (e.g. Yaremych *et al.* 2004). Extending the temporal and spatial model scales would also allow dynamical models to be integrated with statistical environmental models of habitat quality and climate change for more detailed disease forecasting (e.g. Randolph & Rogers 2000; McCallum & Dobson 2002; Rogers *et al.* 2002).

The importance of many additional ecological features of the vectors, reservoirs, and disease, could also be tested. For example, arboviral pathogens can influence vector

behaviour and survival (e.g. Grimstad *et al.* 1980; Moncayo *et al.* 2000; Lacroix *et al.* 2005) in ways that have yet to be incorporated into these models. The importance of disease transmission horizontally among reservoir individuals (Kuno 2001) and through secondary hosts (Higgs *et al.* 2005) should also be evaluated.

Although arboviral models thus far have generally been developed to consider single generic species, empirical studies show that parameter values can vary among interacting vector species (e.g. Turell *et al.* 2001; Goddard *et al.* 2002; Tiawsirisup *et al.* 2004, 2005), host species (e.g. Bernard *et al.* 2001; Komar *et al.* 2003) and viral strains (e.g. Brault *et al.* 2004; Langevin *et al.* 2005). The effect on $\mathcal{R}_0$ of modelling multiple species (e.g. Choi *et al.* 2002; Dobson 2004), including vector biting preference for different host stages and species (e.g. Lord & Day 2001a,b; Apperson *et al.* 2004) also warrants further investigation. Mathematically, most of the existing models use constant rate parameters for transition from one population class to the next. This standard mathematical simplification can underestimate $\mathcal{R}_0$ (Wearing *et al.* 2005), and its importance for host–vector systems should be established.

These environmental and ecological factors scale up to the evolutionary level, where mosquito hybridization (Fonseca *et al.* 2004), coevolution among viruses, vectors and hosts (Anderson & Roitberg 1999; Myers *et al.* 2000; Grenfell *et al.* 2004) and the interactive effects of multiple diseases (e.g. Hunter *et al.* 2003; Rohani *et al.* 2003) all play out. Although these extensions inevitably increase model complexity and reduce tractability, it remains important to assess their relative roles in linking disease dynamics and control at local and global scales.

ACKNOWLEDGEMENTS

REFERENCES

Anderson, R.M. & May, R.M. (1991) *Infectious Diseases of Humans.* Oxford University Press, Oxford.

Anderson, R. & Roitberg, B. (1999) Modeling feeding persistence in mosquitoes. *Ecol. Lett.*, 2, 98–105.

Apperson, C.S., Hassan, H.K., Harrison, B.A., Savage, H.M., Aspen, S.E., Farajollahi, A. *et al.* (2004) Host feeding patterns of established and potential mosquito vectors of West Nile virus in the eastern United States. *Vector Borne Zoonotic Dis.*, 4, 71–82.

Begon, M., Bennett, M., Bowers, R.G., French, N.P., Hazel, S.M. & Turner J. (2002) A clarification of transmission terms in host-microparasite models: numbers, densities and areas. *Epidemiol. Infect.*, 129, 147–153.

Bernard, K.A., Maffei, J.G., Jones, S.A., Kauffman, E.B., Ebel, G.D., Dupuis, A.P. Jr *et al.* (2001) West Nile virus infection in birds and mosquitoes, New York State, 2000. *Emerg. Infect. Dis.*, 7, 679–685

Blower, S.M. & Dowlatabadi, H. (1994) Sensitivity and uncertainty analysis of complex models of disease transmission: an HIV model, as an example. *Int. Stat. Rev.*, 62, 229–243.

Bowman, C., Gumel, A.B., den Driessche, P., Wu, J. & Zhu, H. (2005) A mathematical model for assessing control strategies against West Nile virus. *Bull. Math. Biol.*, 67, 1107–1133.

Brault, A.C., Langevin, S.A., Bowen, R.A., Panella, N.A., Biggerstaff, B.J., Miller, B.R. *et al.* (2004) Differential virulence of West Nile strains for American crows. *Emerg. Infect. Dis.*, 10, 2161–2168.

Castillo-Chavez, C., with Blower, S., van den Driessche, P., Kirschner, D. & Yakubu, A.-A. (2002) *Mathematical Approaches for Emerging and Reemerging Infectious Diseases: An Introduction.* Springer, New York.

Choi, Y.J., Comiskey, C., Lindsay, M.D., Cross, J.A. & Anderson, M. (2002) Modelling the transmission dynamics of Ross River virus in southwestern Australia. *IMA J. Math. Appl. Med.*, 19, 61–74.

Chomel, B.B. (2003) Control and prevention of emerging zoonoses. *J. Vet. Med. Educ.*, 30, 145–147.

Chowell, G., Castillo-Chavez, C., Fenimore, P.W., Kribs-Zaleta, C.M., Arriola, L. & Hyman, J.M. (2004) Model parameters and outbreak control for SARS. *Emerg. Infect. Dis.*, 10, 1258–1263.

Cruz-Pacheco, G., Esteva, L., Montano-Hirose, J.A. & Vargas, C. (2005) Modelling the dynamics of West Nile virus. *Bull. Math. Biol.*, 67, 1157–1172.

Darensburg, T. & Kocic, V.L. (2004) On the discrete model of West Nile-like epidemics. *Proc. Dyn. Sys. Appl.* 4, 358–366.

Daszak, P., Cunningham, A.A. & Hyatt, A.D. (2000) Emerging infectious diseases of wildlife-threats to biodiversity and human health. *Science*, 287, 443–449.

Diekmann, O. & Heesterbeek H. (2000) *Mathematical Epidemiology of Infectious Diseases.* Wiley, Chichester, UK.

Dobson, A. (2004) Population dynamics of pathogens with multiple host species. *Am. Nat.*, 164, S64–S78.

Dobson, A. & Foufopoulos, J. (2001) Emerging infectious pathogens of wildlife. *Philos. Trans. R. Soc. B*, 356, 1001–1012.

van den Driessche, P. & Watmough, J. (2002) Reproduction numbers and sub-threshold endemic equilibria for compartmental models of disease transmission. *Math. Biosci.*, 180, 29–48.

Enserink, M. (2004) Emerging infectious diseases – a global fire brigade responds to disease outbreaks. *Science*, 303, 1605–1606.

Fonseca, D.M., Keyghobadi, N., Malcolm, C.A., Mehmet, C., Schaffner, F., Mogi, M. *et al.* (2004) Emerging vectors in the *Culex pipiens* complex. *Science*, 303, 1535–1538.

Getz, W.M. & Pickering, J. (1983) Epidemic models: thresholds and population regulation. *Am. Nat.*, 121, 892–898.

Ghosh, A.K. & Tapaswi, P.K. (1999) Dynamics of Japanese Encephalitis – a study in mathematical epidemiology. *IMA J. Math. Appl. Med. Biol.*, 16, 1–27.

Glass, K. (2005) Ecological mechanisms that promote arbovirus survival: a mathematical model of Ross River virus transmission. *Trans. R. Soc. Trop. Med. Hyg.*, 99, 252–260.

Goddard, L.B., Roth, A.E., Reisen, W.K. & Scott, T.W. (2002) Vector competence of California mosquitoes for West Nile virus. *Emerg. Infect. Dis.*, 8, 1385–1391.

Grenfell, B.T., Pybus, O.G., Gog, J.R., Wood, J.L.N., Daly, J.M., Mumford, J.A. *et al.* (2004) Unifying the epidemiological and evolutionary dynamics of pathogens. *Science*, 303, 327–332.

Grimstad, P.R., Ross, Q.E. & Craig, G.B. Jr (1980) *Aedes triseriatus* (Diptera: Culicidae) and La Crosse virus II. Modification of mosquito feeing behavior by virus infection. *J. Med. Entomol.*, 17, 1–7.

Gubler, D.J. (2002) The global emergence/resurgence of arboviral diseases as public health problems. *Arch. Med. Res.*, 33, 330–342.

Gubler, D.J., Campbell, G.L., Nasci, R., Komar, N., Petersen, L. & Roehrig, J.T. (2000) West Nile virus in the United States: guidelines for detection, prevention, and control. *Viral Immunol.*, 13, 469–475.

Hastings, A., Cuddington, K., Davies, K.F., Dugaw, C.J., Elmendorf, S., Freestone, A. *et al.* (2005) The spatial spread of invasions: new developments in theory and evidence. *Ecol. Lett.*, 8, 91–101.

Heesterbeek, H. (2002) A brief history of $\mathcal{R}_0$ and a recipe for its calculation. *Acta Biotheor.*, 50, 189–204.

Heffernan, J.M., Smith, R.J. & Wahl, L.M. (2005) Perspectives on the basic reproductive ratio. *J. R. Soc. Interface*, 2, 281–293.

Hethcote, H.W. (2000) The mathematics of infectious diseases. *SIAM Rev.*, 42, 599–653.

Higgs, S., Schneider, B.S., Vanlandingham, D.L., Klingler, K.A. & Gould, E.A. (2005) Nonviremic transmission of West Nile virus. *Proc. Natl Acad. Sci. USA*, 102, 8871–8874.

Hosseini, P.R., Dhondt, A.A. & Dobson, A. (2004) Seasonality and wildlife disease: how seasonal birth, aggregation and variation in immunity affect the dynamics of *Mycoplasma gallisepticum* in house finches. *Proc. R. Soc. Lond. B*, 271, 2569–2577.

Hunter, P.R., Chalmers, R.M., Syed, Q., Hughes, L.S., Woodhouse, S. & Swift, L. (2003) Foot and mouth disease and cryptosporidiosis: possible interaction between two emerging infectious diseases. *Emerg. Infect. Dis.*, 9, 109–112.

Kay, B.H., Saul, A.J. & McCullagh, A. (1987) A mathematical model for the rural amplification of Murray Valley encephalitis-virus in southern Australia. *Am. J. Epidemiol.*, 125, 690–705.

Keeling, M.J. (2005) Extensions to mass-action mixing. In: *Ecological Paradigms Lost: Routes of Theory Change* (eds Cuddington, K. & Beisner, B.E.). Elsevier, Burlington, MA, pp. 107–142.

Koelle, K. & Pascual, M. (2004) Disentangling extrinsic from intrinsic factors in disease dynamics: a nonlinear time series approach with an application to cholera. *Am. Nat.*, 163, 901–913.

Komar, N., Langevin, S., Hinten, S., Nemeth, N., Edwards, E., Hettler, D. *et al.* (2003) Experimental infection of North American birds with the New York 1999 strain of West Nile virus. *Emerg. Infect. Dis.*, 9, 311–322.

Komar, N., Panella, N.A., Langevin, S., Brault, A.C., Amador, M., Edwards, E. *et al.* (2005) Avian hosts for West Nile virus in St. Tammany parish, Louisiana, 2002. *Am. J. Trop. Med. Hyg.*, 73, 1031–1037.

Kuno, G. (2001) Transmission of arboviruses without involvement of arthropod vectors. *Acta Virol.*, 45, 139–150.

Lacroix, R., Mukabana, W.R., Gouagna, L.C. & Koella, J.C. (2005) Malaria infection increases attractiveness of humans to mosquitoes. *PLoS Med.*, 3, 1590–1593.

Langevin, S.A., Brault, A.C., Panella, N.A., Bowen, R.A. & Komar, N. (2005) Variation in virulence of West Nile virus strains for house sparrows (*Passer domesticus*). *Am. J. Trop. Med. Hyg.*, 72, 99–102.

Lewis, M.A., Rencławowicz, J. & van den Driessche, P. (2006a) Travelling waves and spread rates for a West Nile virus model. *Bull. Math. Biol.* (in press). DOI: 10.1007/s11538-005-9018-x

Lewis, M.A., Rencławowicz, J., van den Driessche, P. & Wonham, M.J. (2006b) A comparison of continuous and discrete time West Nile virus models. *Bull. Math. Biol.* (in press). DOI: 10.1007/s11538-005-9039-x

Lord, C.C. & Day, J.F. (2001a) Simulation studies of St. Louis Encephalitis virus in South Florida. *Vector Borne Zoonotic Dis.*, 1, 299–315.

Lord, C.C. & Day, J.F. (2001b) Simulation studies of St. Louis Encephalitis and West Nile viruses: the impact of bird mortality. *Vector Borne Zoonotic. Dis.*, 1, 317–329.

McCallum, H. & Dobson, A. (2002) Disease, habitat fragmentation and conservation. *Proc. R. Soc. Lond. B*, 269, 2041–2049.

McCallum, H., Barlow, N. & Hone, J. (2001) How should pathogen transmission be modelled? *Trends Ecol. Evol.*, 16, 295–300.

Moncayo, A.C., Edman, J.D. & Turell, M.J. (2000) Effect of eastern equine encephalomyelitis virus on the survival of *Aedes albopictus*, *Anopheles quadrimaculatus*, and *Coquillettidia perturbans* (Diptera: Culicidae). *J. Med. Entomol.*, 37, 701–706.

Myers, M.F., Rogers, D.J., Cox, J., Flahault, A. & Hay, S.I. (2000) Forecasting disease risk for increased epidemic preparedness in public health. *Adv. Parasitol.*, 47, 309–330.

Pascual, M. & Dobson, A. (2005) Seasonal patterns of infectious diseases. *PLoS Med.*, 2, 18–20.

Peterson, A.T., Komar, N., Komar, O., Navarro-Siguenza, A., Robbins, M.B. & Martinez-Meyer, E. (2004) West Nile virus in the New World: potential impacts on bird species. *Bird Conserv. Int.*, 14, 215–232.

Randolph, S.E. & Rogers, D.J. (2000) Satellite data and vector-borne infections: mapping risk prediction. *Bull. Soc. Pathol. Exot.*, 93, 207.

Rogers, D.J., Randolph, S.E., Snow, R.W. & Hay, S.I. (2002) Satellite imagery in the study and forecast of malaria. *Nature*, 415, 710–715.

Rohani, P., Green, C.J., Mantilla-Beniers, N.B. & Grenfell, B.T. (2003) Ecological interference between fatal diseases. *Nature*, 422, 885–888.

Rudolf, V.H.W. & Antonovics, J. (2005) Species coexistence and pathogens with frequency-dependent transmission. *Am. Nat.*, 166, 112–118.

Sanchez, M.A. & Blower, S.M. (1997) Uncertainty and sensitivity analysis of the basic reproductive rate: tuberculosis as an example. *Am. J. Epidemiol.*, 145, 1127–1137.

Saul, A. (2003) Zooprophylaxis or zoopotentiation: the outcome of introducing animals on vector transmission is highly dependent on the mosquito mortality while searching. *Malaria J.*, 2, 32.

Saul, A.J., Graves, P.M. & Kay, B.H. (1990) A cyclical feeding model for pathogen transmission and its application to

determine vectorial capacity from vector infection rates. *J. Appl. Ecol.*, 27, 123–133.

Shaman, J., Day, J.F. & Stieglitz, M. (2002) Drought-induced amplification of Saint Louis encephalitis virus, Florida. *Emerg. Infect. Dis.*, 8, 575–580.

Tapaswi, P.K., Ghosh, A.K. & Mukhopadhyay, B.B. (1995) Transmission of Japanese encephalitis in a 3-population model. *Ecol. Model.*, 83, 295–309.

Thomas, D.M. & Urena, B. (2001) A model describing the evolution of West Nile-like encephalitis in New York City. *Math. Comput. Model.*, 34, 771–781.

Thrall, P.H., Antonovics, J. & Hall, D.W. (1993) Host and pathogen coexistence in sexually transmitted and vector-borne diseases characterized by frequency-dependent disease transmission. *Am. Nat.*, 142, 543–552.

Tiawsirisup, S., Platt, K.B., Evans, R.B. & Rowley, W.A. (2004) Susceptibility of *Ochlerotatus trivittatus*(Coq.), *Aedes albopictus* (Skuse), and *Culex pipiens*(L.) to West Nile virus infection. *Vector Borne Zoonotic. Dis.*, 4, 190–197.

Tiawsirisup, S., Platt, K.B., Evans, R.B. & Rowley, W.A. (2005) A comparison of West Nile virus transmission by *Ochlerotatus trivittatus* (Coq.), *Culex pipiens* (L.), and *Aedes albopictus* (Skuse). *Vector Borne Zoonotic Dis.*, 5, 40–47.

Turell, M.J., O'Guinn, M.L., Dohm, D.J. & Jones, J.W. (2001) Vector competence of North American mosquitoes (Diptera: Culicidae) for West Nile virus. *J. Med. Entomol.*, 38, 130–134.

Wearing, H.J., Rohani, P. & Keeling, M.J. (2005) Appropriate models for the management of infectious diseases. *PLoS Med.*, 2, 621–627.

Wonham, M.J., de-Camino-Beck, T. & Lewis, M.A. (2004) An epidemiological model for West Nile virus: invasion analysis and control applications. *Proc. R. Soc. Lond. B*, 271, 501–507.

Wood, S.N. & Thomas, M.B. (1999) Super-sensitivity to structure in biological models. *Proc. R. Soc. Lond. B*, 266, 565–570.

Yaremych, S.A., Novak, R.J., Raim, A.J., Mankin, P.C. & Warner, R.E. (2004) Home range and habitat use by American Crows in relation to transmission of West Nile Virus. *Wilson Bull.*, 116, 232–239.

PARAMETER ESTIMATION SOURCES FOR TABLES 2 AND 3

Brault, A.C., Langevin, S.A., Bowen, R.A., Panella, N.A., Biggerstaff, B.J., Miller, B.R. *et al.* (2004) Differential virulence of West Nile strains for American crows. *Emerg. Infect. Dis.*, 10, 2161–2168.

Bugbee, L.M. & Forte, L.R. (2004) The discovery of West Nile Virus in overwintering *Culex pipiens* (Diptera: Culicidae) mosquitoes in Lehigh County, Pennsylvania. *J. Am. Mosquito Control Assoc.*, 20, 326–327.

Colton, L., Biggerstaff, B.J., Johnson, A. & Nasci, R.S. (2005) Quantification of West Nile virus in vector mosquito saliva. *J. Am. Mosquito Control Assoc.*, 21, 49–53.

Dohm, D.J., Sardelis, M.R. & Turell, M.J. (2002) Experimental vertical transmission of West Nile virus by *Culex pipiens* (Diptera: Culicidae). *J. Med. Entomol.*, 39, 640–644.

Dyer, N.I., Pinowski, J. & Pinowska, B. (1977) Population dynamics. In: *Granivorous Birds in Ecosystems* (eds Pinowski, J. & Kendeigh, S.C.). Cambridge University Press, Cambridge, pp. 53-105.

Goddard, L.B., Roth, A.E., Reisen, W.K. & Scott, T.W. (2002) Vector competence of California mosquitoes for West Nile virus. *Emerg. Infect. Dis.*, 8, 1385–1391.

Goddard, L.B., Roth, A.E., Reisen, W.K. & Scott, T.W. (2003) Vertical transmission of West Nile virus by three California *Culex* (Diptera: Culicidae) species. *J. Med. Entomol.*, 40, 743–746.

Griffith, J.S.R. & Turner, G.D. (1996) Culturing *Culex quinquefasciatus* mosquitoes with a blood substitute diet for the females. *Med. Vet. Entomol.*, 10, 265–268.

Hayes, J. & Hsi, B.P. (1975) Interrelationships between selected meteorologic phenomena and immature stages of *Culex pipiens quinquefasciatus* Say: study of an isolated population. *J. Med. Entomol.*, 12, 299–308.

Hickey, M.B. & Brittingham, M.C. (1991) Population dynamics of blue jays at a bird feeder. *Wilson Bull.*, 103, 401–414.

Komar, N., Langevin, S., Hinten, S., Nemeth, N., Edwards, E., Hettler, D. *et al.* (2003) Experimental infection of North American birds with the New York 1999 strain of West Nile virus. *Emerg. Infect. Dis.*, 9, 311–322.

Komar, N., Panella, N.A., Langevin, S., Brault, A.C., Amador, M., Edwards, E. & *et al.* (2005) Avian hosts for West Nile virus in St. Tammany parish, Louisiana, 2002. *Am. J. Trop. Med. Hyg.* (in press).

Langevin, S.A., Brault, A.C., Panella, N.A., Bowen, R.A. & Komar, N. (2005) Variation in virulence of West Nile virus strains for house sparrows (*Passer domesticus*). *Am. J. Trop. Med. Hyg.*, 72, 99–102.

Milby, M.M. & Wright, M.E. (1976) Survival of house sparrows and house finches in Kern County, California. *Bird Banding*, 47, 119–122.

Moncayo, A.C., Edman, J.D. & Turell, M.J. (2000) Effect of eastern equine encephalomyelitis virus on the survival of *Aedes albopictus*, *Anopheles quadrimaculatus*, and *Coquillettidia perturbans* (Diptera: Culicidae). *J. Med. Entomol.*, 37, 701–706.

Mpho, M., Callaghan, A. & Holloway, G.J. (2002) Temperature and genotypic effects on life history and fluctuating asymmetry in a field strain of *Culex pipiens*. *Heredity*, 88, 307–312.

Oda, T., Uchida, K., Mori, A., Mine, M., Eshita, Y., Kurokawa, K. *et al.* (1999) Effects of high temperature on the emergence and survival of adult *Culex pipiens molestus* and *Culex quinquefasciatus* in Japan. *J. Am. Mosquito Control Assoc.*, 15, 153–156.

Reisen, W.K., Fang, Y. & Martinez, V.M. (2005) Avian host and mosquito (Diptera : Culicidae) vector competence determine the efficiency of West Nile and St. Louis encephalitis virus transmission. *J. Med. Entomol.*, 42, 367–375.

Sardelis, M.R. & Turell, M.J. (2001) *Ochlerotatus j. japonicus* in Frederick County, Maryland: discovery, distribution, and vector competence for West Nile virus. *J. Am. Mosquito Control Assoc.*, 17, 137–141.

Suleman, M. & Reisen, W.K. (1979) *Culex quinquefasciatus* Say: life table characteristics of adults reared from wild-caught pupae from North West Frontier Province, Pakistan. *Mosq. News*, 39, 756–762.

Tiawsirisup, S., Platt, K.B., Evans, R.B. & Rowley, W.A. (2004) Susceptibility of *Ochlerotatus trivittatus* (Coq.), *Aedes albopictus*

(Skuse), and *Culex pipiens* (L.) to West Nile virus infection. *Vector Borne Zoonotic Dis.*, 4, 190–197.

Tiawsirisup, S., Platt, K.B., Evans, R.B. & Rowley, W.A. (2005) A comparison of West Nile virus transmission by *Ochlerotatus trivittatus* (Coq.), *Culex pipiens* (L.), and *Aedes albopictus* (Skuse). *Vector Borne Zoonotic Dis*, 5, 40-47.

Turell, M.J., O'Guinn, M.L. & Oliver, J. (2000) Potential for New York mosquitoes to transmit West Nile virus. *Am. J. Trop. Med. Hyg.*, 62, 413–414.

Turell, M.J., O'Guinn, M.L., Dohm, D.J. & Jones, J.W. (2001) Vector competence of North American mosquitoes (Diptera: Culicidae) for West Nile virus. *J. Med. Entomol.*, 38, 130–134.

Vanlandingham, D.L., Schneider, B.S., Klingler, K.A., Fair, J., Beasley, D., Huang, J., Hamilton, P. & Higgs, S. (2004) Real-time reverse transcriptase-polymerase chain reaction quantification of West Nile virus transmitted by *Culex pipiens quinquefasciatus*. *Am. J. Trop. Med. Hyg.*, 71, 120–123.

Walter, N.M. & Hacker, C.S. (1974) Variation in life table characteristics among three geographic strains of *Culex pipiens quinquefasciatus*. *J. Med. Entomol.*, 11, 541–550.

Work, T.H., Hurlbut, H.S. & Taylor, R.M. (1955) Indigenous wild birds of the Nile Delta as potential West Nile virus circulating reservoirs. *Am. J. Trop. Med. Hyg.*, 4, 872–888.

APPENDIX

Here we summarize the formulation and analysis of the seven arboviral encephalitis models treated in this review. For all models, we present the vector and reservoir equations using the common notation in Table 2. We also calculate the basic reproduction number $\mathcal{R}_0$ following the next-generation matrix method (Diekmann & Heesterbeek 2000; van den Driessche & Watmough 2002). (Although convention dictates the use of a different symbol for the reproduction number when a model explicitly includes control, we use $\mathcal{R}_0$ throughout for all models.) We include the calculation details only for models in which $\mathcal{R}_0$ has not previously been reported in the literature from this method. For the other models, we simply give the formula and the reference. For simplicity of $\mathcal{R}_0$ calculation, we treat all rate parameters in the original equations as constants. Although this approach leads to some simplification of the original models, particularly WN1 and JE, it allows a comparison of their basic structures. At the DFE in all models, $I_i = E_i = R_i = 0$, $S_V = N_V = N_V^*$, and $S_R = N_R = N_R^*$.

WN1 (simplified model II from Lord & Day 2001a,b)

These two papers model a single West Nile virus season in Florida, with vectors and juvenile and adult reservoirs. The model is extensively parameterized to allow seasonal variation in environmental factors, which influence mosquito population dynamics, feeding preference, and bird reproductive success and age structure. This is the only

study to conduct a statistical analysis of parameter intercorrelation and model sensitivity. However, $\mathcal{R}_0$ is not calculated and the full system appears too complex for theoretical stability analysis. The same model is also applied to St Louis encephalitis by setting reservoir mortality to zero.

Vectors (Lord & Day 2001a, equation 5):

$$
\begin{aligned}
\frac{dS_V}{dt} &= a_V - \alpha_V\left(\frac{\beta_r I_r}{N_r} + \frac{\beta_R I_R}{N_R}\right)S_V - d_V S_V \\
\frac{dE_V}{dt} &= \alpha_V\left(\frac{\beta_r I_r}{N_r} + \frac{\beta_R I_R}{N_R}\right)S_V - (\kappa_V + d_V)E_V \quad (1.1) \\
\frac{dI_V}{dt} &= \kappa_V E_V - d_V I_V
\end{aligned}
$$

Reservoirs (Lord & Day 2001a, p. 304):

$$
\begin{aligned}
\frac{dS_r}{dt} &= a_r - \alpha_r\beta_r\frac{S_r}{N_r}I_V - (d_r + m_r)S_r \\
\frac{dS_R}{dt} &= m_r S_r - \alpha_R\beta_R\frac{S_R}{N_R}I_V - d_R S_R \\
\frac{dI_i}{dt} &= \alpha_i\beta_i\frac{S_i}{N_i}I_V - (d_i + \delta_i + \gamma_i)I_i, \quad i = r, R \\
\frac{dR_R}{dt} &= \gamma_r I_r + \gamma_R I_R - d_R R_R
\end{aligned}
$$

$$(1.2)$$

This model treats birds that are more susceptible (juvenile, subscript r) and less susceptible (adult, subscript R) separately in compartments S_i and I_i, where $i = r, R$. In the original, the parameters β_i are functions of juvenile and adult reservoir abundances and mosquito preference, d_V and κ_V are linear functions of temperature, which is a cosine function of time, and a_V and a_r are environmentally forced functions of time. The parameter m_r is originally a time delay function accounting for the survival and maturation of uninfected juvenile birds to adults. We inserted the parameter δ_i into the equations dI_i/dt as per the text and figures in Lord & Day (2001b), and made two minor notational corrections: in the original equation for dJ_i/dt we replaced $m_J J_s$ with $m_J J_i$ (which in our notation is $d_r I_r$), and in the original equation for dA_{in}/dt we replaced $r_A A_s$ with $r_A A_{in}$ (which in our notation is $\gamma_R I_R$).

Under the simplifying assumption that all parameters are constant per capita rates, the DFE $(S_V, E_V, I_V, S_r, S_R, I_r, I_R, R_R) = (N_V^*, 0, 0, N_r^*, N_R^*, 0, 0, 0)$ or for the simpler case where all birds are adults $(S_V, E_V, I_V, S_R, I_R, R_R) = (N_V^*, 0, 0, N_R^*, 0, 0)$, where $N_V^* = a_V/d_V$ and $N_i^* = a_i/d_i$. Then $\mathcal{R}_0$ is calculated as follows. The infected equations for $E_V, I_V, I_r,$ and I_R can be rewritten in matrix form, separating new infection terms (f) from vital dynamics terms (v):

$$
\begin{bmatrix} E_V \\ I_V \\ I_r \\ I_R \end{bmatrix}_t = f - v = \begin{bmatrix} \alpha_V(\beta_r I_r/N_r + \beta_R I_R/N_R)S_V \\ 0 \\ \alpha_r \beta_r I_V S_r/N_r \\ \alpha_R \beta_R I_V S_R/N_R \end{bmatrix}
$$
$$
- \begin{bmatrix} (d_V + \kappa_V)E_V \\ -\kappa_V E_V + d_V I_V \\ (d_r + \delta_r + \gamma_r)I_R \\ (d_R + \delta_R + \gamma_R)I_R \end{bmatrix}. \tag{1.3}
$$

Calculating the respective linearized matrices at the DFE gives:

$$
F = \begin{bmatrix} 0 & 0 & \alpha_V \beta_r N_V^*/N_r^* & \alpha_V \beta_R N_V^*/N_R^* \\ 0 & 0 & 0 & 0 \\ 0 & \alpha_r \beta_r & 0 & 0 \\ 0 & \alpha_R \beta_R & 0 & 0 \end{bmatrix}, \tag{1.4}
$$

$$
V = \begin{bmatrix} d_V + \kappa_V & 0 & 0 & 0 \\ -\kappa_V & d_V & 0 & 0 \\ 0 & 0 & d_r + \delta_r + \gamma_r & 0 \\ 0 & 0 & 0 & d_R + \delta_R + \gamma_R \end{bmatrix}. \tag{1.5}
$$

Thus,

$$
V^{-1} = \begin{bmatrix} 1/(d_V + \kappa_V) & 0 & 0 & 0 \\ \kappa_V/[d_V(d_V + \kappa_V)] & 1/d_V & 0 & 0 \\ 0 & 0 & 1/(d_r + \delta_r + \gamma_r) & 0 \\ 0 & 0 & 0 & 1/(d_R + \delta_R + \gamma_R) \end{bmatrix} \tag{1.6}
$$

and the next generation matrix is

$$
FV^{-1} = \begin{bmatrix} 0 & 0 & \frac{\alpha_V \beta_r N_V^*}{(d_r + \delta_r + \gamma_r)N_r^*} & \frac{\alpha_V \beta_R N_V^*}{(d_R + \delta_R + \gamma_R)N_R^*} \\ 0 & 0 & 0 & 0 \\ \frac{\alpha_r \beta_r \kappa_V}{d_V(d_V + \kappa_V)} & \frac{\alpha_r \beta_r}{d_V} & 0 & 0 \\ \frac{\alpha_R \beta_R \kappa_V}{d_V(d_V + \kappa_V)} & \frac{\alpha_R \beta_R}{d_V} & 0 & 0 \end{bmatrix}. \tag{1.7}
$$

There is a double zero eigenvalue of FV^{-1} and the remaining two eigenvalues satisfy a quadratic, so the spectral radius of FV^{-1} is

$$
R_0 = \sqrt{\frac{\varphi_V \alpha_V N_V^*}{d_V}\left(\frac{\alpha_r \beta_r^2}{(d_r + \delta_r + \gamma_r)N_r^*} + \frac{\alpha_R \beta_R^2}{(d_R + \delta_R + \gamma_R)N_R^*}\right)}. \tag{1.8}
$$

This can be compared with $\mathcal{R}_0$ in eqn 10. For a homogeneous reservoir population where all birds are adults, the expression reduces to

$$
R_0 = \sqrt{\frac{\varphi_V \alpha_R \beta_R}{d_V}\frac{\alpha_V \beta_R N_V^*}{(d_R + \delta_R + \gamma_R)N_R^*}}, \tag{1.9}
$$

which can be compared with text eqn 6.

WN2 (based on Thomas & Urena 2001 rewritten as the ODE system in Lewis *et al.* 2006b)

This West Nile virus model was originally formulated as a system of discrete-time difference equations. The model incorporates vectors, reservoirs and humans, and evaluates the effects of periodic spraying as a mosquito control measure. Theoretical model analysis provides parameter ranges on the amount of spraying needed to force the mosquito population to die out, but $\mathcal{R}_0$ is not calculated. Numerical simulations are provided using unspecified parameter values. This continuous-time formulation from Lewis *et al.* (2006b) of the discrete-time model (Thomas & Urena 2001) omits the original mosquito spraying parameter $c(t)$.

Vectors:

$$
\frac{dS_V}{dt} = b_V[S_V + (1 - \rho_V)(E_V + I_V)] - \beta_R' I_R S_V - d_V S_V
$$
$$
\frac{dE_V}{dt} = b_V \rho_V(E_V + I_V) + \beta_R' I_R S_V - (d_V + \kappa_V)E_V
$$
$$
\frac{dI_V}{dt} = \kappa_V E_V - d_V I_V. \tag{2.1}
$$

Reservoirs:

$$
\frac{dS_R}{dt} = b_R N_R - \beta_R' S_R I_V - d_R S_R
$$
$$
\frac{dI_R}{dt} = \beta_R' S_R I_V - (d_R + \gamma_R)I_R \tag{2.2}
$$
$$
\frac{dR_R}{dt} = \gamma_R I_R - d_R R_R.
$$

For $0 < \rho_V \leq 1$, this model incorporates vertical disease transmission in the vector population. The DFE with parameter constraints $b_V = d_V$ and $b_R = d_R$ is $(S_V, E_V, I_V, S_R, I_R, R_R) = (N_V^*, 0, 0, N_R^*, 0, 0)$. The basic reproduction number is

$$R_0 = \sqrt{\frac{\varphi_V \beta_R'}{d_V} \frac{\beta_R' N_V^* N_R^*}{(d_R + \gamma_R)}} \quad \text{for } \rho_V = 0 \qquad (2.3)$$

and

$$\frac{\rho_V}{2} + \sqrt{\left(\frac{\rho_V}{2}\right)^2 + \frac{\varphi_V \beta_R'}{d_V} \frac{\beta_R' N_V^* N_R^*}{(d_R + \gamma_R)}} \quad \text{for } \rho_V > 0, \qquad (2.4)$$

as calculated in Lewis *et al.* (2006b). These can be compared with $\mathcal{R}_0$ in text eqns 3 and 6. The behaviour of the original model with different mosquito-spraying functions is explored by Darensburg & Kocic (2004).

WN3 (Wonham *et al.* 2004)

This model characterizes vector and reservoir populations in a single West Nile virus season in North America. The model is analysed theoretically to obtain disease-free equilibria, evaluate local stability and calculate $\mathcal{R}_0$. Parameter values are obtained from the literature, the model is validated using reported outbreak data, and numerical simulations are shown. Model extensions are presented to calculate threshold mosquito densities for outbreak and to consider seasonal variation in mosquito levels. The model structure, excluding the original equation for dead birds which does not influence the dynamics, is as follows.

Vectors:

$$\frac{dL_V}{dt} = b_L N_V - (m_L + d_L)L_V$$

$$\frac{dS_V}{dt} = -\alpha_V \beta_R \frac{I_R}{N_R} S_V + m_L L_V - d_V S_V$$

$$\frac{dE_V}{dt} = \alpha_V \beta_R \frac{I_R}{N_R} S_V - (\kappa_V + d_V)E_V \qquad (3.1)$$

$$\frac{dI_V}{dt} = \kappa_V E_V - d_V I_V.$$

Reservoirs:

$$\frac{dS_R}{dt} = -\alpha_R \beta_R \frac{S_R}{N_R} I_V$$

$$\frac{dI_R}{dt} = \alpha_R \beta_R \frac{S_R}{N_R} I_V - (\delta_R + \gamma_R)I_R \qquad (3.2)$$

$$\frac{dR_R}{dt} = \gamma_R I_R.$$

The parameter constraint for a constant mosquito population $b_L = d_V(m_L + d_I)/m_L$ gives the DFE as $(L_V, S_V, E_V, I_V, S_R, I_R, R_R) = (d_V N_V^*/m_L, N_V^*, 0, 0, N_R^*, 0, 0)$. The disease basic reproduction number is

$$R_0 = \sqrt{\frac{\varphi_V \alpha_R \beta_R}{d_V} \frac{\alpha_V \beta_R N_V^*}{(\delta_R + \gamma_R)N_R^*}}, \qquad (3.3)$$

as calculated in Wonham *et al.* (2004). Compare text eqn 6.

WN4 (Bowman *et al.* 2005)

This model treats a single West Nile season in North America for vectors, reservoirs and humans. The authors evaluate preventive strategies (mosquito spraying vs. personal prevention) using a detailed representation of five human classes. The model is analysed theoretically to obtain disease-free and endemic equilibria, evaluate local and global stability, and calculate $\mathcal{R}_0$. Numerical results are also shown.

Vectors:

$$\frac{dS_V}{dt} = a_V - \alpha_V \beta_R \frac{I_R}{N_R} S_V - d_V S_V$$

$$\frac{dI_V}{dt} = \alpha_V \beta_R \frac{I_R}{N_R} S_V - d_V I_V. \qquad (4.1)$$

Reservoirs

$$\frac{dS_R}{dt} = a_R - \alpha_R \beta_R \frac{S_R}{N_R} I_V - d_R S_R$$

$$\frac{dI_R}{dt} = \alpha_R \beta_R \frac{S_R}{N_R} I_V - (d_R + \delta_R)I_R. \qquad (4.2)$$

In this model, the mosquito biting rate β_R is initially presented as a general function of the total mosquito, bird and human populations, and later is assumed for simplicity to be a constant rate parameter. The system has a unique DFE, namely $(S_V, I_V, S_R, I_R) = (N_V^*, 0, N_R^*, 0)$, where $N_V^* = a_V/d_V$ and $N_R^* = a_R/d_R$. The disease basic reproduction number is

$$R_0 = \sqrt{\frac{\alpha_R \beta_R}{d_V} \frac{\alpha_V \beta_R N_V^*}{(d_R + \delta_R)N_R^*}}, \qquad (4.3)$$

as calculated in Bowman *et al.* (2005); compare text eqn 6.

WN5 (Cruz-Pacheco *et al.* 2005)

This West Nile virus model is analysed theoretically to obtain disease-free and endemic equilibria and to evaluate local stability and, for the case of no reservoir-induced disease mortality, global stability. The authors define an expression for $\mathcal{R}_0$, which is then compared for eight North

American bird species. Numerical outbreak simulations are also shown for different species.

Vectors:

$$\frac{dS_V}{dt} = b_V[S_V + (1 - \rho_V)I_V] - \alpha_V\beta_R\frac{I_R}{N_R}S_V - d_VS_V$$

$$\frac{dI_V}{dt} = \rho_Vb_VI_V + \alpha_V\beta_R\frac{I_R}{N_R}S_V - d_VI_V.$$

(5.1)

Reservoirs:

$$\frac{dS_R}{dt} = a_R - \alpha_R\beta_R\frac{S_R}{N_R}I_V - d_RS_R$$

$$\frac{dI_R}{dt} = \alpha_R\beta_R\frac{S_R}{N_R}I_V - (d_R + \delta_R + \gamma_R)I_R$$

$$\frac{dR_R}{dt} = \gamma_RI_R - d_RR_R.$$

(5.2)

The DFE is $(S_V, I_V, S_R, I_R, R_R) = (N_V^*, 0, N_R^*, 0, 0)$, where $N_R^* = a_R/d_R$ and the vector vital rates $b_V = d_V$. We recalculate $\mathcal{R}_0$ from the infected equations for I_V and I_R written as

$$\begin{bmatrix} I_V \\ I_R \end{bmatrix}_t = f - v = \begin{bmatrix} \alpha_V\beta_RI_RS_V/N_R + \rho_Vb_VI_V \\ \alpha_R\beta_RI_VS_R/N_R \end{bmatrix} - \begin{bmatrix} d_VI_V \\ (d_R + \delta_R + \gamma_R)I_R \end{bmatrix}.$$

(5.3)

Consequently,

$$F = \begin{bmatrix} \rho_Vd_V & \alpha_V\beta_RN_V^*/N_R^* \\ \alpha_R\beta_R & 0 \end{bmatrix} \quad \text{and}$$

$$V = \begin{bmatrix} d_V & 0 \\ 0 & d_R + \delta_R + \gamma_R \end{bmatrix}$$

(5.4)

so that

$$FV^{-1} = \begin{bmatrix} \rho_V & \alpha_V\beta_RN_V^*/(d_R + \delta_R + \gamma_R)N_R^* \\ \alpha_R\beta_R/d_V & 0 \end{bmatrix}.$$

(5.5)

The spectral radius is then

$$R_0 = \frac{\rho_V}{2} + \sqrt{\left(\frac{\rho_V}{2}\right)^2 + \frac{\alpha_R\beta_R}{d_V}\frac{\alpha_V\beta_RN_V^*}{(d_R + \delta_R + \gamma_R)N_R^*}};$$

(5.6)

compare text eqn 7. The expression for $\mathcal{R}_0$ obtained by our method differs from that of the corresponding term $\tilde{R}_0$ defined in Cruz-Pacheco *et al.* (2005), p. 1170). This difference arises when ρ_V is correctly treated as causing new infections and therefore entering in *f*, rather than as a vital rate term appearing in *v* (see van den Driessche &

Watmough 2002). When we set $\rho_V = 0$, both $\mathcal{R}_0$ above and $\tilde{R}_0$ reduce to

$$R_0 = \sqrt{\frac{\alpha_R\beta_R}{d_V}\frac{\alpha_V\beta_RN_V^*}{(d_R + \delta_R + \gamma_R)N_R^*}}.$$

(5.7)

JE (simplified from Tapaswi *et al.* 1995)

Japanese encephalitis is a mosquito-borne arbovirus endemic to southeast Asia. It differs from West Nile virus in having important mammalian as well as bird reservoirs, and in not causing reservoir mortality. This model of JE in India includes vectors, reservoirs, and humans. It is analysed theoretically to obtain disease-free and endemic equilibria, discuss local and global stability, and calculate $\mathcal{R}_0$. The reservoir–human subset of this model is simulated numerically in Ghosh & Tapaswi (1999).

Vectors:

$$\frac{dS_V}{dt} = a_V + \eta_VI_V - \alpha_V\beta_RI_R\frac{S_V}{N_V} - d_VS_V$$

$$\frac{dI_V}{dt} = \alpha_V\beta_RI_R\frac{S_V}{N_V} - (d_V + \eta_V)I_V.$$

(6.1)

Reservoirs:

$$\frac{dS_R}{dt} = b_RN_R + \eta_RR_R - \alpha_R\beta_R\frac{S_R}{N_R}I_V - d_RS_R$$

$$\frac{dI_R}{dt} = \alpha_R\beta_R\frac{S_R}{N_R}I_V - (d_R + \gamma_R)I_R$$

$$\frac{dR_R}{dt} = \gamma_RI_R - (d_R + \eta_R)R_R.$$

(6.2)

In JE the original vector recruitment term $a_V = (b_V - (b_V - d_V)N_V/K_V)N_V$, where K_V is the carrying capacity of adult mosquitoes. Under the simplifying assumption that a_V is a constant rate parameter, the DFE is $(S_V, I_V, S_R, I_R, R_R) = (N_V^*, 0, N_R^*, 0, 0)$, where $N_V^* = K_V$ and the reservoir birth and death rates are assumed to be equal.

The $\mathcal{R}_0$ defined in Tapaswi *et al.* (1995, p. 298) corresponds to our R_0^2, which we calculate from the infected equations written as

$$\begin{bmatrix} I_V \\ I_R \end{bmatrix}_t = f - v = \begin{bmatrix} \alpha_V\beta_RI_RS_V/N_V \\ \alpha_R\beta_RI_VS_R/N_R \end{bmatrix} - \begin{bmatrix} (d_V + \eta_V)I_V \\ (d_R + \gamma_R)I_R \end{bmatrix}.$$

(6.3)

Consequently,

$$F = \begin{bmatrix} 0 & \alpha_V\beta_R \\ \alpha_R\beta_R & 0 \end{bmatrix} \quad \text{and} \quad V = \begin{bmatrix} d_V + \eta_V & 0 \\ 0 & d_R + \gamma_R \end{bmatrix}$$

(6.4)

so that

$$FV^{-1} = \begin{bmatrix} 0 & \alpha_V\beta_R/(d_R+\gamma_R) \\ \alpha_R\beta_R/(d_V+\eta_V) & 0 \end{bmatrix}. \quad (6.5)$$

The spectral radius is then

$$R_0 = \sqrt{\frac{\alpha_R\beta_R}{(d_V+\eta_V)}\frac{\alpha_V\beta_R}{(d_R+\gamma_R)}}; \quad (6.6)$$

compare text eqns 4 and 6.

RR (Simplified from Choi *et al.* 2002)

Ross River virus is the most common mosquito-borne arbovirus in Australia. The majority of hosts are marsupials. This model considers Western Gray kangaroo reservoirs and humans, and is the only one of the seven arboviral models to incorporate two different vector species. Since the disease is endemic, disease transmission incorporates the added parameter ψ_V, which accounts for vectors newly infected by reservoirs other than kangaroos and humans.

As the two sets of vector equations are identical, we show just one for ease of model comparison.

Vectors:

$$\frac{dS_V}{dt} = a_V - \alpha_V\beta'_R I_V S_V - (d_V+\psi_V)S_V$$

$$\frac{dE_V}{dt} = (\alpha_V\beta'_R I_V + \psi_V)S_V - (d_V+\kappa_V)E_V. \quad (7.1)$$

$$\frac{dI_V}{dt} = \kappa_V E_V - d_V I_V$$

Reservoirs (kangaroos):

$$\frac{dS_R}{dt} = -\alpha_R\beta'_R S_R I_V$$

$$\frac{dI_R}{dt} = \alpha_R\beta'_R S_R I_V - \gamma_R I_R. \quad (7.2)$$

The original study presents numerical simulations and analytical disease outbreak thresholds, but $\mathcal{R}_0$ cannot be calculated because there is no DFE. To allow the basic model structure to be compared, we set $\psi_V = 0$ and assume $N_V^* = a_V/d_V$, giving the DFE as $(S_V, I_V, E_V, I_R, R_R) = (N_V^*, 0, 0, N_R^*, 0)$. The equations for infected individuals are then

$$\begin{bmatrix} E_V \\ I_V \\ I_R \end{bmatrix}_t = f - v = \begin{bmatrix} \alpha_V\beta'_R I_R S_V \\ 0 \\ \alpha_R\beta'_R I_V S_R \end{bmatrix} - \begin{bmatrix} (d_V+\kappa_V)E_V \\ -\kappa_V E_V + d_V I_V \\ \gamma_R I_R \end{bmatrix}. \quad (7.3)$$

Consequently,

$$F = \begin{bmatrix} 0 & 0 & \alpha_V\beta'_R N_V^* \\ 0 & 0 & 0 \\ 0 & \alpha_R\beta'_R N_R^* & 0 \end{bmatrix}$$

$$V = \begin{bmatrix} d_V+\kappa_V & 0 & 0 \\ -\kappa_V & d_V & 0 \\ 0 & 0 & \gamma_R \end{bmatrix}. \quad (7.4)$$

The next generation matrix is then

$$FV^{-1} = \begin{bmatrix} 0 & 0 & \frac{\alpha_V\beta'_R N_V^*}{\gamma_R} \\ 0 & 0 & 0 \\ \frac{\alpha_R\beta'_R \kappa_V N_R^*}{d_V(d_V+\kappa_V)} & \frac{\alpha_R\beta'_R N_R^*}{d_V} & 0 \end{bmatrix}, \quad (7.5)$$

with spectral radius

$$R_0 = \sqrt{\frac{\varphi_V\alpha_R\beta'_R}{d_V}\frac{\alpha_V\beta'_R N_V^* N_R^*}{\gamma_R}}; \quad (7.6)$$

compare text eqns 3 and 6.